5.4 Groundwater Level

The groundwater level was investigated on the basis of 5.1.3 (FIG. V-1) and 5.2 (FIG. V-2, V-3 and V-4).

In 5.2, it was explained that a linear relationship was obtained for the difference between the groundwater level and the elevation on the deep well and shallow well maps. The distance to the points plotted from the 45° line on the map is thought to be the groundwater.

In the northern sector, determining the average water level for each elevation gave those depths within approximately 110m (average 50m), and those between 150 - 160m, with the water level of the deepest ones being near to EL 1300m. The former may possibly indicate free aquifer (unconfined aquifers), and the latter show lower aquifers having the character of confined aquifers.

The groundwater level in the southern sector has depths of less than 120m (average 70m), and depths between 150 - 180m. Therefore, there are also several artesian wells in the Ojo de Agua sector, and their water level is around EL 1300m. It is therefore concluded that both free aquifers and lower aquifers exist in the southern sector. (see FIG. V-6)

The eastern sector has many extremely shallow pump-up wells and many of these have groundwater levels of less than 50m. Unlike the two sectors described above, this is thought to show that groundwater is being taken from a free aquifer. Furthermore, many of those with depths below around EL 1300m lie on the 45° line, and are thought to indicate surface artesian flow of the lower aquifer.

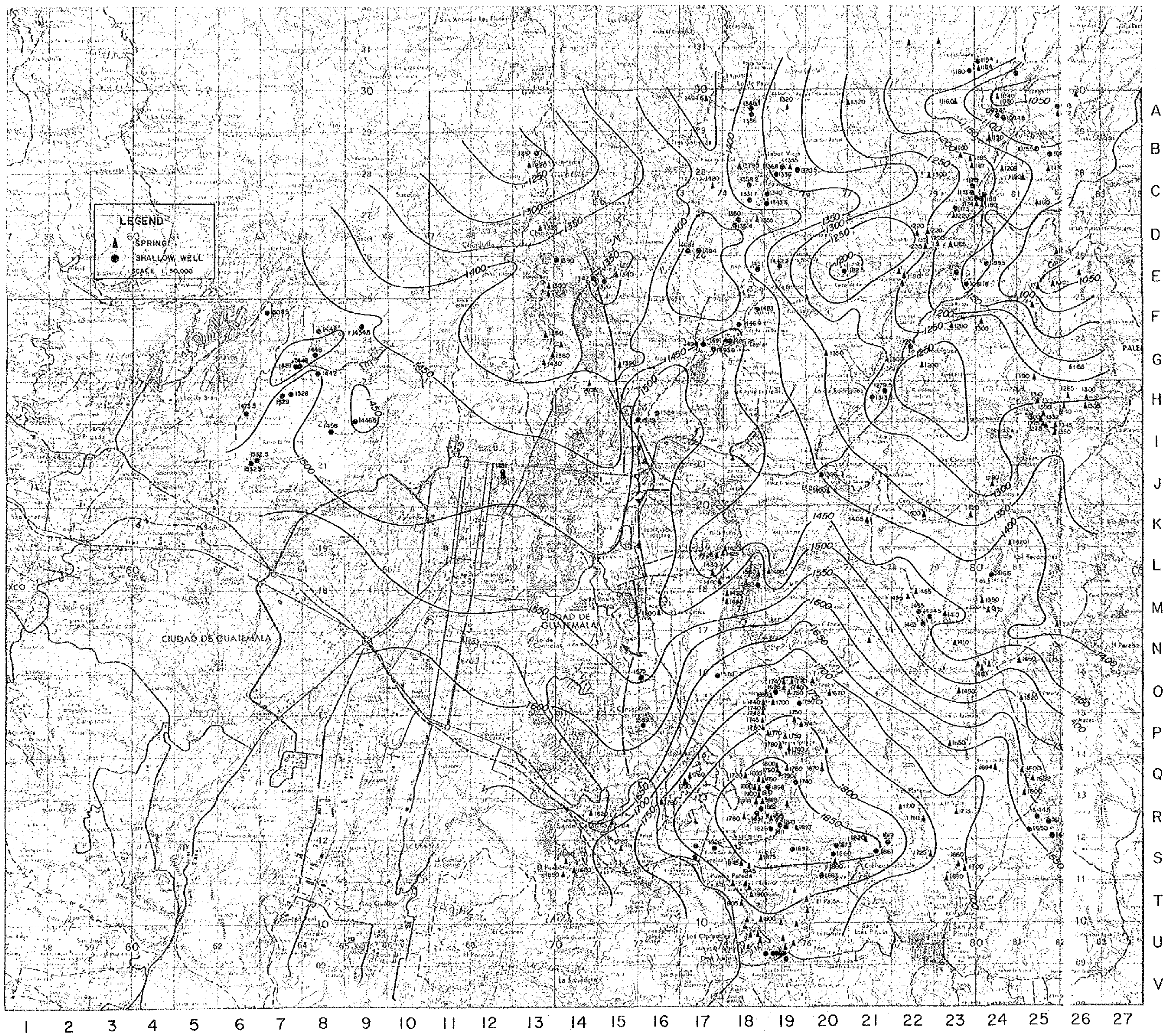

FIG. V-1 ISOGRAPHY OF FREE WATER TABLE (UNCONFINED GROUNDWATER)

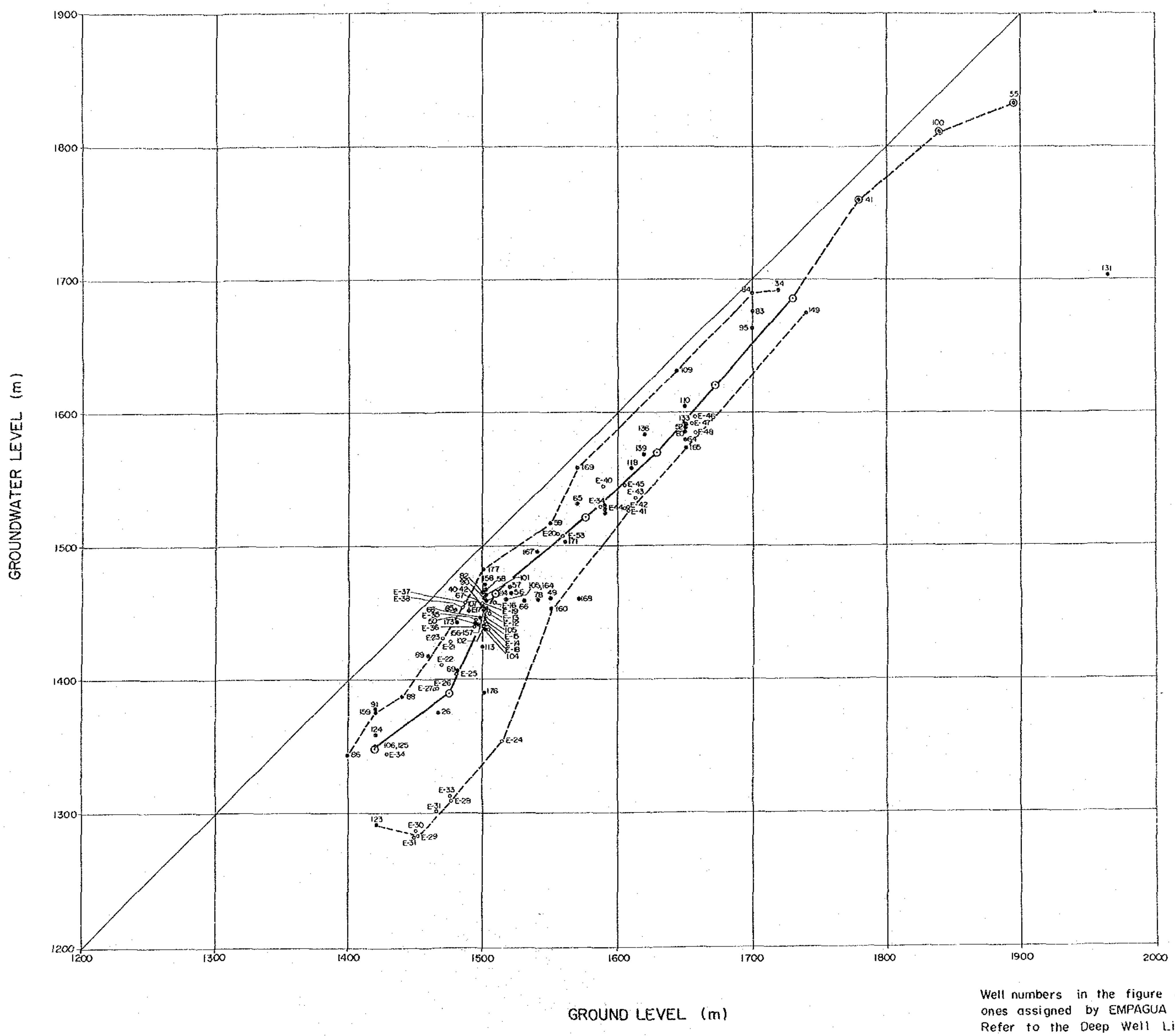

FIG. V-2 DIAGRAM OF GROUNDWATER LEVEV & GROUND LEVEL (DEEPWELLS OF NORTHERN AREA)

Well numbers in the figure are previous ones assigned by EMPAGUA and INSIVUMEH. Refer to the Deep Well List for new well numbers assigned under the study (Previous well numbers are given in the remarks column). well numbers in FIG. V-5 are newly assigned under the study.

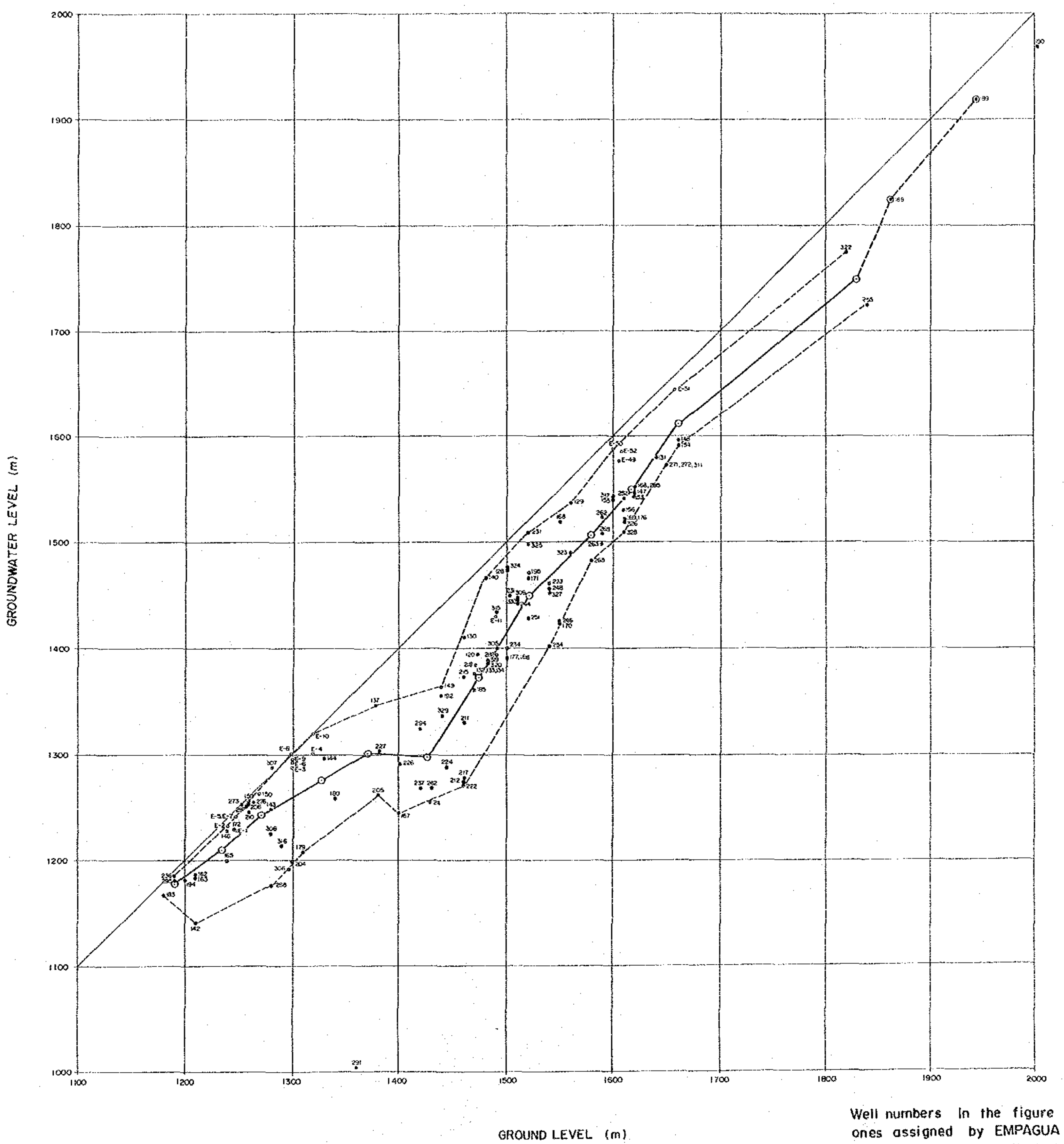

FIG. V-3 DIAGRAM OF GROUNDWATER LEVEL & GROUND LEVEL
(DEEPWELLS OF SOUTHERN AREA)

Well numbers in the figure are previous ones assigned by EMPAGUA and INSIVUMEH. Refer to the Deep Well List for new well numbers assigned under the study (Previous well numbers are given in the remarks column). well numbers in FIG. V-5 are newly assigned under the study.

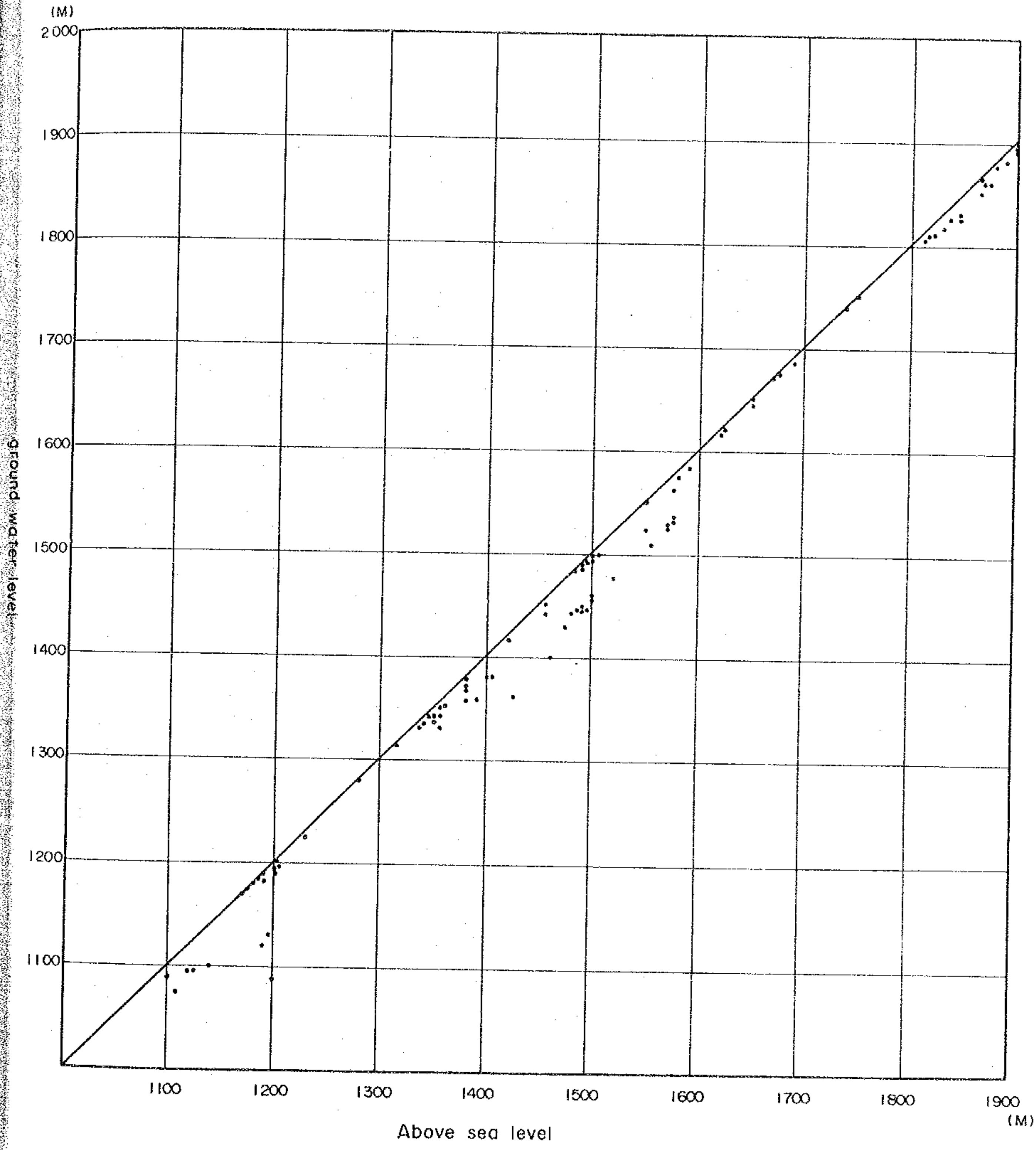

FIG.V-4. DIAGRAM OF GROUND WATER LEVEL AND GROUND LEVEL (SHALLOW WELLS)

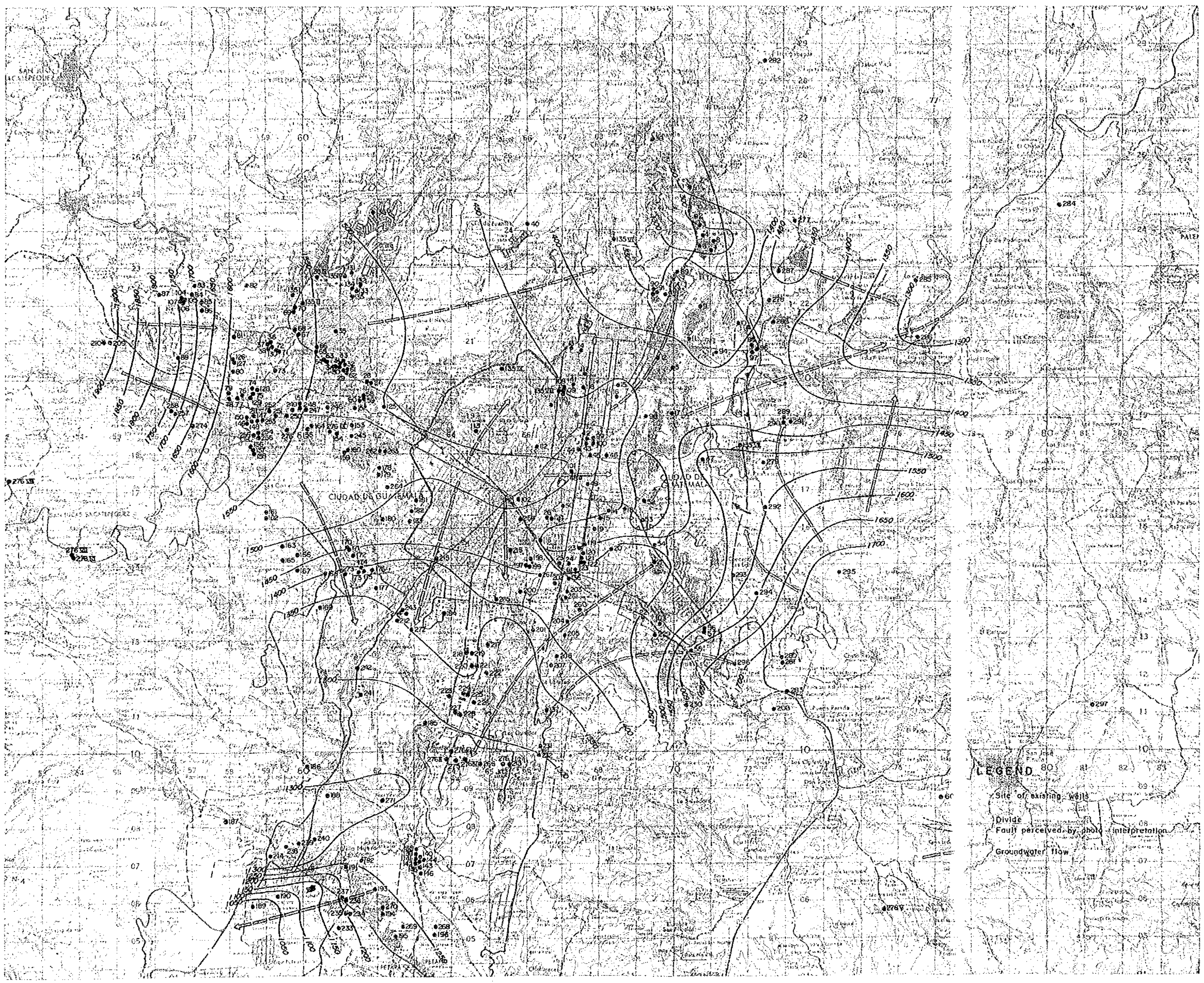

FIG. V-5 GROUNDWATER FLOW REGIME

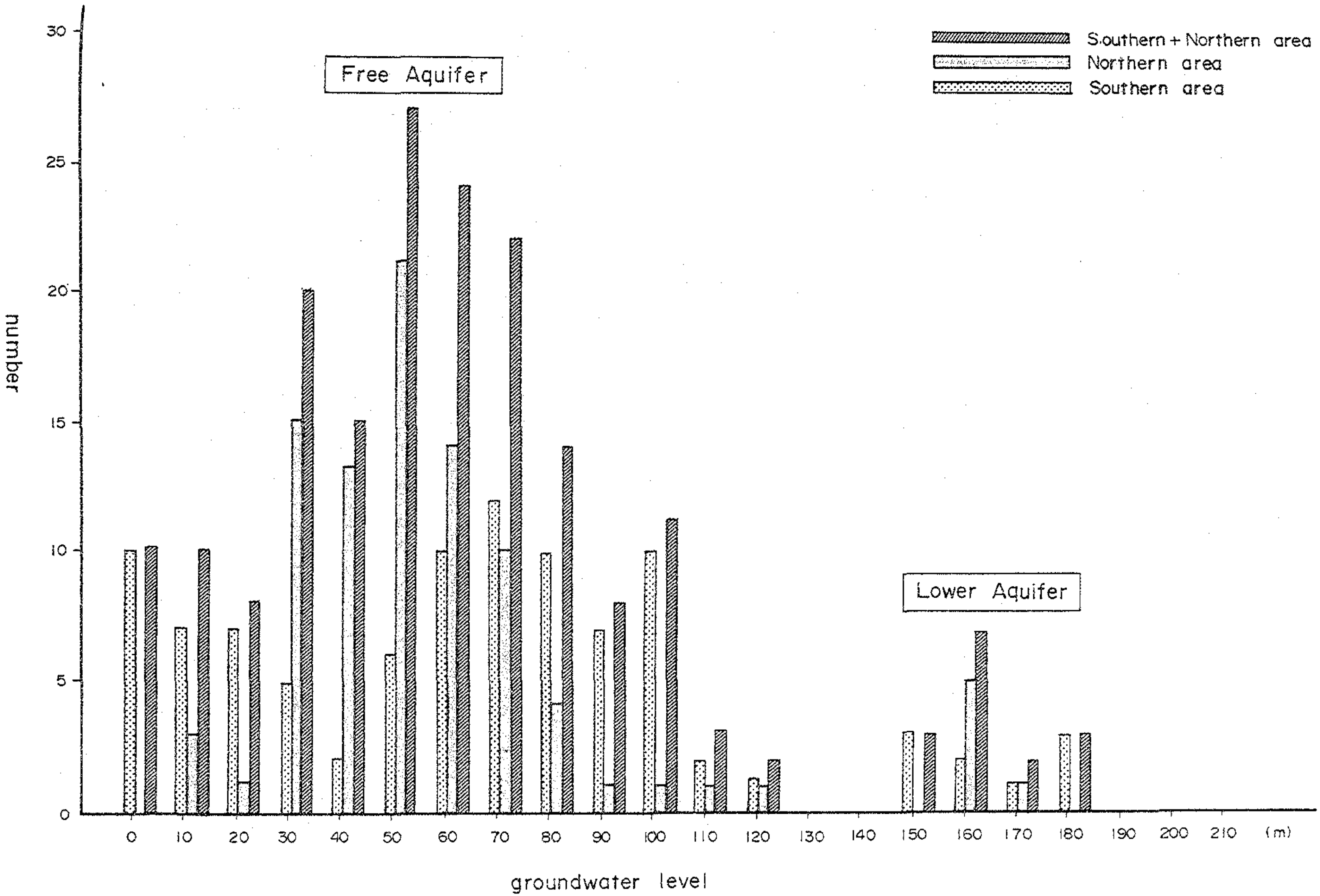

Fig. V-6 Frequency distribution of groundwater level

TABLE V-1 FREE AQUIFER CHARACTERISTICS

Location	Elevation	Groundwater Level Elevation	Temper-ature T°C	pH	Conductivity	Comments
A-17	1,495	1,495.5		6.0	120.0μ s/cm	spring
A-18	1,380	1,356		7.0	330.0μ s/cm	shallow well
A-18	1,380	1,368.1		6.5	370.0μ s/cm	"
A-19	1,320	1,320		6.0	170.0μ s/cm	spring
A-20	1,320	1,320		6.0	130.0μ s/cm	"
A-23	1,116	1,116	23.1	6.5	124.2μ s/cm	"
A-24	1,124	1,094.8	24.0	6.5	300.0μ s/cm	shallow well
A-24	1,120	1,093.3	25.0	7.0	300.0μ s/cm	"
A-24	1,040	1,040		7.5	190.0μ s/cm	spring
A-23	1,180	1,180	24.5	7.0	128.8μ s/cm	shallow well
A-24	1,200	1,194	24.6	6.0	100.0μ s/cm	"
A-24	1,185	1,184	28.8	7.5	130.5μ s/cm	lake
A-25	1,183	1,183	24.0	6.0	-----	shallow well
A-25	1,182	1,182	28.0	7.0	-----	lake
A-24	1,140	1,100	25.6	7.0	-----	shallow well
B-13	1,210	1,210		8.0	280.0μ s/cm	"
B-13	1,220	1,210		6.5	320.0μ s/cm	spring
B-18	1,380	1,379.5		6.5	150.0μ s/cm	"
B-19	1,340	1,336.8		6.0	350.0μ s/cm	shallow well
B-19	1,355	1,355		6.0	250.0μ s/cm	spring
B-10	1,400	1,380	23.7	6.5	142.8μ s/cm	shallow well
B-19	1,380	1,370.5		6.5	230.0μ s/cm	shallow well
B-23	1,180	1,180		7.0	84.0μ s/cm	spring
B-23	1,185	1,185	22.0	6.0	282.0μ s/cm	"
B-23	1,187	1,187	26.0	5.5	97.8μ s/cm	"
B-24	1,208	1,208	24.0	6.5	125.0μ s/cm	"
B-24	1,150	1,150	24.5	6.5	130.0μ s/cm	"
B-25	1,130	1,130	26.0	6.0	63.0μ s/cm	"
B-25	1,108	1,075.5	25.0	7.5	-----	shallow well
B-25	1,108	1,090	---	--	-----	"

TABLE V-1 FREE AQUIFER CHARACTERISTICS

Location	Elevation	Groundwater Level Elevation	Temperature T°C	pH	Conductivity	Comments
B-10	1,400	1,380	23.5	6.5	140.3μ s/cm	"
C-17	1,420	1,420		5.5	210.0μ s/cm	spring
C-18	1,395	1,358.2		6.5	250.0μ s/cm	shallow well
C-18	1,335	1,331.7		7.0	350.0μ s/cm	"
C-19	1,350	1,336		7.0	210.0μ s/cm	"
C-19	1,350	1,340		6.5	100.0μ s/cm	"
C-19	1,350	1,343.8		7.5	530.0μ s/cm	"
C-22	1,300	1,300	20.5	7.5	129.0μ s/cm	spring
C-23	1,190	1,118	23.6	6.5	149.5μ s/cm	shallow well
C-23	1,175	1,175	24.3	5.5	136.5μ s/cm	"
C-23	1,175	1,175	22.1	6.5	98.6μ s/cm	"
C-10	1,340	1,340	19.0	7.5	154.2μ s/cm	spring
C-10	1,340	1,340	18.1	8.0	119.7μ s/cm	spring
C-24	1,188	1,188	23.0	8/0	458.0μ s/cm	shallow well
C-24	1,196	1,130	23.0	7.5	632.0μ s/cm	"
C-24	1,180	1,180	24.0	6.0	399.0μ s/cm	spring
C-24	1,179	1,179	22.0	7/0	350.0μ s/cm	"
C-24	1,200	---	23.2	6.5	243.0μ s/cm	shallow well
C-25	1,110	1,110	24.5	6.0	156.0μ s/cm	spring
C-25	1,190	1,190	25.0	6.0	42.0μ s/cm	"
C-9	1,380	1,380	18.9	8.5	140.0μ s/cm	"
D-13	1,325	1,325		7.0	180.0μ s/cm	spring
D-17	1,500	1,494		8.0	320.0μ s/cm	shallow well
D-17	1,490	1,488.9		5.5	140.0μ s/cm	"
D-18	1,355	1,355		7.5	420.0μ s/cm	spring
D-18	1.355	1,350		6.0	75.0μ s/cm	shallow well
D-18	1,355	1,351.4		6.0	61.0μ s/cm	"
D-22	1,220	1,220	23.7	6.5	100.0μ s/cm	spring
D-22	1,220	1,220	22.8	6.0	195.9μ s/cm	"
D-22	1,235	1,235	27.1	5.5	176.6μ s/cm	"

TABLE V-1 FREE AQUIFER CHARACTERISTICS

Location	Elevation	Groundwater Level Elevation	Temper- ature T°C	pH	Conductivity	Comments
D-23	1,200	1,200	23.5	6.0	101.1μ s/cm	"
D-23	1,220	1,220	25.1	6.0	92.0μ s/cm	"
D-23	1,185	1,185	22.8	6.0	195.9μ s/cm	"
D-11	1,350	1,350	19.4	7.5	140.0μ s/cm	"
D-10	1,450	1,360	21.8	7.0	155.8μ s/cm	shallow well
D-2.5	1,135	1,035		8.5	390.0μ s/cm	spring
D-10	1,450	1,400	22.3	6.5	166.0μ s/cm	"
E-13	1,325	1,325		7.0	350.0μ s/cm	"
E-13	1,300	1,300		7.5	83.0μ s/cm	"
E-14	1,350	1,342		8.0	430.0μ s/cm	shallow well
E-14	1,405	1,390		6.5	250.0μ s/cm	spring
E-15	1,340	1,340		6.0	250.0μ s/cm	spring
E-15	1,355	1,328		6.0	250.0μ s/cm	shallow well
E-18	1,455	1,451.0		7.0	310.0μ s/cm	"
E-19	1,455	1,442.20		8.0	600.0μ s/cm	"
E-20	1,190	1,182.5		7.5	430.0μ s/cm	"
E-22	1,180	1,180		7.0	530.0μ s/cm	spring
E-23	1,200	1,196		7.5	700.0μ s/cm	shallow well
E-23	1,200	1,084.18		6.5	150.0μ s/cm	"
E-24	1,200	1,189.50		6.0	410.0μ s/cm	"
E-25	1,040	1,040	28.2	7.0	400.0μ s/cm	spring
F-7	1,555	1,508.5		7.0	250.0μ s/cm	shallow well
F-8	1,490	1,448		7.5	210.0μ s/cm	"
F-9	1,500	1,454.5		7.0	300.0μ s/cm	"
F-13	1,350	1,350		7.5	210.0μ s/cm	spring
F-18	1,485	1,446.9		7.0	920.0μ s/cm	"
F-23	1,280	1,280		6.5	180.0μ s/cm	"
F-24	1,300	1,300		7.0	160.0μ s/cm	"
F-6	1,540					"
G-7	1,475	1,429		6.5	220.0μ s/cm	shallow well

TABLE V-1 FREE AQUIFER CHARACTERISTICS

Location	Elevation	Groundwater Level Elevation	Temper-ature T°C	pH	Conductivity	Comments
G-7	1,490	1,448		6.5	120.0μ s/cm	"
G-8	1,490	1,448		6.5	150.0μ s/cm	"
G-8	1,480	1,442		8.0	210.0μ s/cm	"
G-13	1,430	1,430		6.5	130.0μ s/cm	spring
G-13	1,360	1,360		7.0	230.0μ s/cm	"
G-15	1,390	1,390		6.5	230.0μ s/cm	"
G-17	1,500	1,495.5		5.5	420.0μ s/cm	shallow well
G-17	1,500	1,496		7.0	470.0μ s/cm	"
G-18	1,490	1,486.25		6.5	140.0μ s/cm	"
G-18	1,495	1,491		6.5	690.0μ s/cm	shallow well
G-20	1,350	1,350		8.5	350.0μ s/cm	spring
G-21	1,300	1,300		7.0	230.0μ s/cm	"
G-22	1,200	1,200		8.0	980.0μ s/cm	"
G-22	1,230	1,224		6.5	180.0μ s/cm	shallow well
G-25	1,190	1,190	23.2	5.5	85.4μ s/cm	spring
G-26	1,55	1,155	24.0	5.5	80.1μ s/cm	"
G-14	1,360			8.0	400.0μ s/cm	"
H-6	1,520	1,473.5		7.0	270.0μ s/cm	shallow well
H-7	1,570	1,528		6.0	170.0μ s/cm	"
H-7	1,572	1,529		6.5	180.0μ s/cm	"
H-9	1,490	1,446.5		6.0	190.0μ s/cm	"
H-14	1,405	1,405		7.5	320.0μ s/cm	spring
H-16	1,550	1,549		6.0	390.0μ s/cm	shallow well
H-16	1,550	1,524.0		8.0	600.0μ s/cm	"
H-21	1,315	1,313.3		8.5	1,200.0μ s/cm	"
H-21	1,280	1,279.5		6.5	500.0μ s/cm	"
H-25	1,310	1,310	21.5	6.5	119.5μ s/cm	spring
H-25	1,3000	1,300	20.7	8.0	145.3μ s/cm	"
H-26	1,265	1,265	25.0	5.5	75.0μ s/cm	"
H-26	1,300	1,300	25.1	5.5	93.3μ s/cm	"

TABLE V-1 FREE AQUIFER CHARACTERISTICS

Location	Elevation	Groundwater Level Elevation	Temper-ature T°C	pH	Conductivity	Comments
H-26	1,305	1,305	26.5	5.5	97.1μ s/cm	"
H-26	1,340	1,340	23.6	6.0	183.7μ s/cm	"
I-9	1,420	1,420	20.6	6.5	169.1μ s/cm	spring
I-6	1,575	1,532.5		6.5	130.0μ s/cm	shallow well
I-6	1,575	1,532.5		6.5	190.0μ s/cm	"
I-8	1,500	1,456		7.0	150.0μ s/cm	"
I-25	1,350	1,350	24.5	6.0	192.1μ s/cm	spring
I-25	1,345	1,345	23.0	7.0	216.0μ s/cm	"
I-25	1,275	1,275	25.4	5.5	73.0μ s/cm	"
I-25	1,275	1,275	24.1	7.0	66.5μ s/cm	"
I-25	1,332	1,332	25.6	7.5	79.4μ s/cm	"
I-9	1,420	1,420	21.5	7.0	190.4μ s/cm	"
J-12	1,485	1,481		7.0	430.0μ s/cm	shallow well
J-12	1,485	1,481		7.0	790.0μ s/cm	"
J-20	1,460	1,398		6.0	180.0μ s/cm	"
J-20	1,400	1,400		6.5	62.0μ s/cm	spring
J-24	1,280	1,280				"
J-9	1,420	1,420	17.6	7.0	181.5μ s/cm	"
J-8	1,460	1,460	17.2	8/5	164.9μ s/cm	"
K-21	1,405	1,405		6.5	320.0μ s/cm	spring
K-22	1,400	1,400		6.5	180.0μ s/cm	"
K-23	1,420	1,420		7.0	250.0μ s/cm	"
K-24	1,420	1,420				"
K-17	1,412	1,412	20.9	6.5	43.9μ s/cm	spring
K-18	1,400	1,400	20.4	8.0	123.7μ s/cm	"
K-18	1,376	1,376	19.0	8.5	40.4μ s/cm	"
K-18	1,410	1,410	18.0	8.5	32.4μ s/cm	"
K-18	1,405	1,405	22.8	6.5	43.9μ s/cm	"
K-19	1,480	1,480	20.7	8.5	142.8μ s/cm	"
K-19	1,382	1,380	18.4	7.5	224.0μ s/cm	shallow well

TABLE V-1 FREE AQUIFER CHARACTERISTICS

Location	Elevation	Groundwater Level Elevation	Temper-ature T°C	pH	Conductivity	Comments
L-18	1,560	1,560		6.5	130.0μ s/cm	spring
L-18	1,490	1,488.3		6.0	330.0μ s/cm	shallow well
L-19	1,450	1,450	23.0	6.0	164.6μ s/cm	spring
L-24	1,420	1,417		6.0	30.0μ s/cm	shallow well
L-19	1,518	1,518	22.2	8.5	295.0μ s/cm	spring
M-16	1,500	1,500		6.0	190.0μ s/cm	spring
M-22	1,455	1,455		6.5	150.0μ s/cm	"
M-22	1,455	1,455		6.0	130.0μ s/cm	"
M-22	1,490	1,485		6.0	440.0μ s/cm	shallow well
M-22	1,490	1,484.5		6.0	350.0μ s/cm	"

Location	Elevation	Groundwater Level Elevation	Temperature T°C	pH	Conductivity	Comments
M-22	1,490	1,483.0		6.5	290.0μ s/cm	"
M-23	1,410	1,410		5.5	190.0μ s/cm	spring
M-24	1,410	1,410		6.5	190.0μ s/cm	"
M-24	1,390	1,390		7.0	61.0μ s/cm	"
M-25	1,390	1,390		7.5	130.0μ s/cm	"
N-19	1,575	1,562	24.5	6.5	128.9μ s/cm	shallow well
N-23	1,410	1,410		5.5	130.0μ s/cm	spring
N-24	1,450	1,450		6.5	150.0μ s/cm	"
N-25	1,460	1,460		6.5	130.0μ s/cm	"
N-18	1,580	1,555	25.2	7.5	222.0μ s/cm	
O-16	1,580	1,575		5.5	170.0μ s/cm	shallow well
O-23	1,480	1,480		6.0	80.0μ s/cm	spring
O-25	1,520	1,520		6.5	90.0μ s/cm	"
O-18	1,742	1,742	21.0	7.5	49.3μ s/cm	spring
O-18	1,740	1,740	20.8	8.5	67.6μ s/cm	"
O-18	1,740	1,740	19.3	7.0	121.7μ s/cm	"
O-19	1,750	1,750	20.1	6.5	107.9μ s/cm	"
O-19	1,740	1,740	19.5	6.0	155.2μ s/cm	"
O-19	1,740	1,740	16.5	7.5	63.4μ s/cm	"
O-19	1,760	1,760	18.2	6.0	155.2μ s/cm	"
O-19	1,685	1,685	19.5	6.5	86.5μ s/cm	"
O-19	1,700	1,700	19.6	6.0	89.2μ s/cm	"
O-19	1,690	1,685	19.0	6.5	87.2μ s/cm	shallow well
O-19	1,750	1,750	18.6	6.5	109.5μ s/cm	"
O-20	1,670	1,670				
P-19	1,740	1,740	18.6	6.0	43.7μ s/cm	"
P-16	1,590	1,584.5		6.0	150.0μ s/cm	shallow well
P-23	1,650	1,650		7.5	130.0μ s/cm	spring
P-19	1,770	1,770	19.2	6.0	85.4μ s/cm	"
P-18	1,750	1,750	20.2	6.0	88.5μ s/cm	spring
P-18	1,745	1,745	19.2	6.0	65.9μ s/cm	"
P-19	1,750	1,750	20.5	8.0	71.7μ s/cm	"

Location	Elevation	Groundwater Level Elevation	Temper-ature T°C	pH	Conductivity	Comments
P-19	1,740	1,740	21.6	6.0	62.6μ s/cm	"
P-19	1,750	1,750	18.5	8.5	51.9μ s/cm	"
P-19	1,780	1,780	17.3	6.5	72.4μ s/cm	"
Q-18	1,720	1,720		6.5	100.0μ s/cm	spring
Q-24	1,690	1,690		5.5	93.0μ s/cm	"
Q-25	1,675	1,652		5.5	160.0μ s/cm	shallow well
Q-25	1,600	1,600		6.0	150.0μ s/cm	spring
Q-25	1,600	1,600		6.0	80.0μ s/cm	"
Q-17	1,750	1,750	19.7	7.0	84.7μ s/cm	
Q-17	1,760	1,760	20.1	7.5	76.4μ s/cm	
Q-18	1,910	1,910	21.3	6.3	46.6μ s/cm	
Q-18	1,900	1,900	15.9	7.5	43.4μ s/cm	
Q-18	1,880	1,880	16.8	6.0	52.6μ s/cm	
Q-18	1,88-	1,88-	17.2	8.5	56.9μ s/cm	
Q-18	1,880	1,880	18.7	6.5	67.8μ s/cm	
Q-19	1,890	1,890	17.8	7.5	114.1μ s/cm	
Q-19	1,790	1,790	17.3	7.0	58.1μ s/cm	
Q-19	1,800	1,800	16.6	7.5	57.3μ s/cm	spring
Q-19	1,760	1,760	17.8	8.0	56.1μ s/cm	spring
Q-19	1,741	1,740	18.7	6.0	90.7μ s/cm	shallow well
Q-19	1,900	1,898	17.5	6.0	43.2μ s/cm	shallow well
Q-20	1,670	1,670	18.5	6.5	266.0μ s/cm	spring
R-14	1,620	1,620		6.5	210.0μ s/cm	spring
R-16	1,760	1,760		6.0	310.0μ s/cm	"
R-18	1,760	1,760		6.0	240.0μ s/cm	"
R-22	1,710	1,710		5.5	53.0μ s/cm	"
R-22	1,710	1,710		6.0	88.0μ s/cm	"
R-23	1,715	1,715		6.0	87.0μ s/cm	"
R-25	1,650	1,650		6.0	240.0μ s/cm	shallow well
R-25	1,620	1,617		6.0	240.0μ s/cm	"
R-25	1,620	1,611.5		6.0	230.0μ s/cm	"
R-25	1,650	1,644.5		5.5	150.0μ s/cm	"

Location	Elevation	Groundwater Level Elevation	Temper-ature T°C	pH	Conductivity	Comments
R-18	1,888	1,888	15.4	6.0	73.8μ s/cm	spring
R-18	1,888	1,888	16.0	6.0	70.9μ s/cm	"
R-18	1,865	1,862	17.0	6.5	59.9μ s/cm	shallow well
R-18	1,862	1,851	18.0	6.0	262.0μ s/cm	"
R-19	1,822	1,811	18.2	6.5	905.0μ s/cm	"
R-19	1,835	1,826	19.0	6.5	68.7μ s/cm	"
R-19	1,816	1,810	20.8	5.5	135.4μ s/cm	"
R-19	1,815	1,815	18.8	6.0	67.7μ s/cm	spring
R-19	1,810	1,810	20.7	6.5	120.9μ s/cm	
S-14	1,650	1,650		5.5	95.0μ s/cm	spring
S-14	1,680	1,680		7.0	190.0μ s/cm	"
S-14	1,660	1,660		7.5	120.0μ s/cm	"
S-15	1,720	1,720		6.5	230.0μ s/cm	"
S-17	1,845	1,826	21.1	5.5	161.7μ s/cm	shallow well
S-17	1,840					
S-17	1,840					
S-18	1,875	1,875	20.3	6.5	48.3μ s/cm	spring
S-18	1,845	1,845	21.0	6.5	74.5μ s/cm	"
S-18	1,845	1,845	20.4	6.5	70.1μ s/cm	spring
S-20	1,880	1,880		6.5	180.0μ s/cm	"
S-19	1,900	1,892		5.5	80.0μ s/cm	shallow well
S-20	1,890	1,883		6.0	78.0μ s/cm	"
S-20	1,880	1,873		5.5	240.0μ s/cm	"
S-20	1,870	1,860		5.5	220.0μ s/cm	"
S-21	1,870	1,861		7.0	200.0μ s/cm	"
S-21	1,830	1,819		5.5	90.0μ s/cm	"
S-21	1,820	1,820		7.0	80.0μ s/cm	spring
S-22	1,725	1,725		5.5	73.0μ s/cm	"
S-23	1,660	1,660		7.5	82.0μ s/cm	"
S-23	1,700	1,700		6.0	77.0μ s/cm	"
S-23	1,680	1,680		7.5	130.0μ s/cm	"

CHAPTER VI

GEOPHYSICS

Based on the conclusions of Section 2.5, electrical prospecting was planned in eastern and northern (Cerro el Naranjo) areas of Guatemala city.

Electrical prospecting methods are generally adopted to find ground water veins in the confined aquifer. TABLE VI-1 shows a summary of electrical prospecting methods.

TABLE VI-1 Electrical Methods Utilized

Using polarization	Natural	Self potential method
	Artificial	Frequency induced polarization method
Using resistivity distribution	Natural	Telluric-current method
	Artificial	Resistivity method Equipotential-line method Potential-drop ratio method
	Artificial (Electromagnetic method	Galvanic electromagnetic method Resistivity method

The resistivity method is described below as this was the method actually employed in the subject study.

6.1 Resistivity Method

In reality, the geologic structure of a given land area is seldom homegenous, and generally exhibits extreme complexity. A land area delimited by the horizontal surface is indicated in FIG. VI-1 as a two-layered horizontal structure consisting of a first layer of resistivity p, and thickness d, and a second layer of resistivity p_2 and thickness d_2.

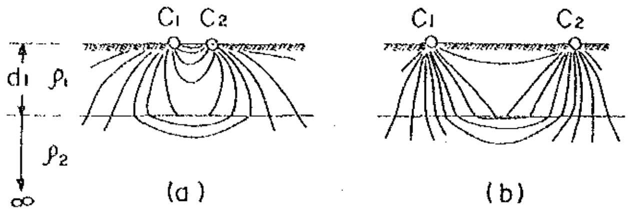

FIG. VI-1 Current Distribution in a Two-Layered Horizontal Structure

When electric current is transmitted from a pair of current electrodes c_1, c_2 on the surface where the interval between c_1 and c_2 is extremely small in relation to the thickness d_1 of the first layer a, since the current emitted from c_1 passes through the second layer before being received by c_2, the recorded resistivity value is ρ_1. As the interval between c_1 and c_2 is steadily increased, the emitted current passes deeper and deeper underground and is subsequently affected by the resistivity ρ_2 of the second layer. In the case of diagram (b) of FIG. VI-1, the impact of the second layer on the recorded resistivity is stronger than in the case of (a). Where the resistivity ρ_2 is greater than that of the first layer, the apparent resisitivity increases; and where $\rho_2 < \rho_1$, the apparent resistivity decreases. As the electrode spacing is steadily increased, the observed apparent resisitivity approaches the value ρ_2.

Establishment of a reference measuring point in this manner, and increasing of the electrode spacing to obtain the vertical apparent resistivity is referred to as the vertical electrical method. Furthermore, movement of electrodes as a pair laterally along a measurement line in order to determine subsurface resistivity at a range of points is referred to as the electrical profiling method.

The two representative techniques generally applied in the vertical electrical method are the Wenner and Schlumberger methods.

6.2 Schlumberger Method

The electrode configuration formula for the Schlumberger method is indicated in FIG. VI-2. In relation to a center point O, potential electrodes p_1 and p_2 are fixed at interval a_1. Current electrodes c_1 and c_2 only are subsequently spaced at increasing intervals centered on point O. In this manner apparent resistivity is measured. However, the condition $\overline{C1C2} \geq \overline{P1P2}$ is stipulated.

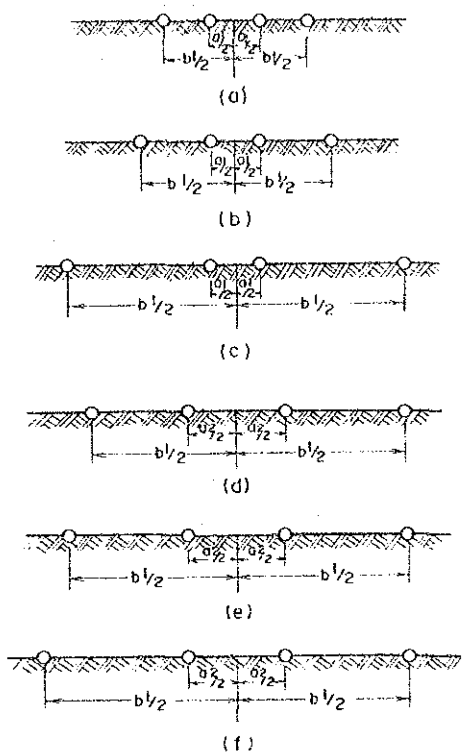

FIG. VI-2 Vertical Electrical Prospecting According to the Schlumberger Method

As spacing of the current electrodes is increased, the difference of potential induced between potential electrodes P_1 and P_2 steadily decreases. As the potential differential between P_1 and P_2 grows smaller and approaches the self potential value, measurement error increases. As a result, before this situation occurs, battery voltage should be raised and ground current increased to minimize measurement error. Furthermore, when spacing between current electrodes exceeds 25 times that of potential electrodes, the interval between P_1 and P_2 should be fixed at an appropriately increased interval (a_2) and measuring procedures continued. When $\overline{C_1 C_2}$ again reaches 25 times a_2, the aforementioned adjustment of P_1, P_2 interval should be repeated. However, resistivity values recorded at $\overline{P_1 P_2} = a_1$ and those recorded of $\overline{P_1 P_2} = a_2$ in relation to a certain interval $\overline{C_1 C_2}$ may differ slightly. Consequently, when the potential electrode spacing is changed, the last 2-3 measurements made with the previous potential electrode spacing (a_1) should be repeated at the new potential electrode spacing (a_2).

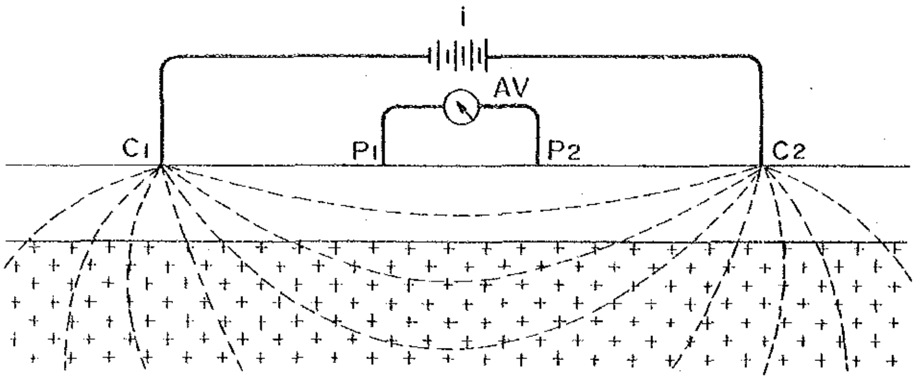

FIG. VI-3 Schlumberger Electrode Configuration

Since electrodes C_1, P_1, P_2, and C_2 are positioned symmertrical to the centerpoint O in FIG. VI-3,

$$\overline{C_1\ P_1} = \overline{C_2\ P_2} \qquad \overline{C_2\ P_1} = \overline{C_1\ P_2}$$

Accordingly,

$$V = \frac{\rho\ I}{\pi}\left(\frac{1}{\overline{C_1\ P_2}} - \frac{1}{\overline{C_1\ P_2}}\right)$$

$$= \frac{\rho\ I}{\pi}\left(\frac{\overline{C_1\ P_2}}{\overline{C_1\ P_2}} - \frac{\overline{C_1\ P_1}}{\overline{C_1\ P_2}}\right)$$

Here,

$$\overline{C_1\ P_1} = \frac{\overline{C_1\ C_2}}{2} - \frac{\overline{P_1\ P_2}}{2}, \quad \overline{C_1\ P_2} = \frac{\overline{C_1\ C_2}}{2} - \frac{\overline{P_1\ P_2}}{2}$$

If the following relationship,

$$\overline{C_1\ P_2} - \overline{C_1\ P_1} = \overline{P_1\ P_2}$$

is inserted in the above formula, then,

$$V = \frac{\rho\ I}{\pi}\left(\frac{4 \cdot \overline{P_1P_2}}{\overline{C_1C_2}^{\,2} \quad \overline{P_1P_2}^{\,2}}\right)$$

Financial calculation is made according to the following formula,

$$\rho = \frac{\pi}{4} \cdot \frac{\overline{C_1 C_1}^2 - \overline{P_1 P_2}^2}{\overline{P_1 P_2}} \cdot \frac{V}{I}$$

Note should be made of the fact that in the case of the Schlumberger method, instead of C_1, C_2, P_1 and P_2 as electrode symbols, A, B, M and N are sometimes used.

6.2.1 Location and Number of Measurements

Measurement locations are as shown in FIG. VI-4, VI-5. Number of measurements were 47 in the eastern sector and 14 in the northern sector (vicinity of Cerro el Naranjo) respectively, for a total of 61 sites.

6.2.2 Current Electrode and Potential Electrode Configuration

Configurations are indicated in TABLE VI-2. The larger the spacing of electrodes C_1 and C_2, the more desirable, as this permitted analysis of ground structure to a greater depth. In the subject investigation, $C_1\ C_2$ = 2000 m was the largest spacing of current electrodes.

6.2.3 Resistivity Method Analysis

Analysis of vertical resistivity sounding is carried out under the premise that ground structure is a horizontal, multilayered one. Analysis accordingly seeks to derive a horizontal, multi-layered structure which produces a theoretical curve most closely resembling the actual measurement curve. Various research has been carried out concerning analysis methods for apparent resistivity curves of horizontal multi-layered structures. Conventionally, the most widely applied method has been curve matching. There are basically too approaches to this method, one of which employs standard curve matchings. The other entails presumption of horizontal multi-layer models from which theoretical curves are derived and compared with actual measurement results. This simulation is repeated until a model is obtained which closely approximates the actual measurement curve. As both approaches to curve matching represent trial and error methods, a certain degree of skill is required to minimize human error.

In addition to the above type of curve matching, automatic analysis through curves applying the method of least squares has begun being employed recently. With this approach, initial values for ρ and a are given and a model derived. Actual measurement and theoretical curves are automatically processed and matched by computer. As a result, the time required for analysis is greatly reduced, and variations according to human error are minimized. Nevertheless, utilization of computer analysis still requires determination of initial ρ and a values. To effectively perform such, a degree of experience is essential.

Curve matching by computer was adopted for the purposes of the subject investigation. Data was processed by Epson HC-20 and NEC PC 9801-M2 personal computers.

6.2.4 VES Curve (Vertical Electric Sounding)

This curve represents the measurement curve for vertical electric sounding of apparent resistivity. In this case logarithmic coordinates are generally applied, with electrode spacing along the horizontal axis and apparent resistivity on the vertical axis. TABLE VI-3 indicates data (point SE-25) obtained from vertical electric sounding. Data was analyzed and simulation performed utilizing a personal computer, and ground structure was projected. The simulation analysis diagram obtained in this manner is given as FIG. VI-6 to VI-15.

The three-layered structure curve exhibits characteristics determined by the inter-relationship of apparent resistivities $_1$, $_2$, and $_3$ for respective layers 1, 2 and 3. On the basis of these relationship, the four following types of curve segments were obtained.

H type: $\rho_1 > \rho_2 < \rho_3$

A type: $\rho_1 < \rho_2 < \rho_3$

K type: $\rho_1 < \rho_2 > \rho_3$

Q type: $\rho_1 > \rho_2 > \rho_3$

TABLE VI-5 indicates recorded survey data.

6.2.5 Interpretation of Schlumberger Method

Interpretation of electrical prospecting data for each prospecting site was completed using personal computers (NEC PC 980-M2, EPSON HC-20). Geological interpretation was made based on resistivity profiles, using as reference the correlation between resistivity and lithology as indicated in TABLE VI-4.

Resistivity log results and ground structure projections based thereon are presented below on a profile-wise basis.

(1) A-A' Profile (see FIG. VI-6)

This profile stretches from west (El Zapote) to east (Lo de Rodrigues).

Analysis of this profile is as below.

Section	Apparent resistivity	Projected ground structure	Comments
1. West of El Marullero river	Surface and shallow layers: < 10 Ω m Deeper layers: 650-2,500 Ω m	Shallow layers are estimated as pyroclastic materials, judging from apparent resistivity values, underlying layers are considered to be andesitic lava and limestone. The north side of SE-24 evidences outcrops of limestone while outcrops of andesitic lava are seen in the south. Comparison of apparent resistivities for SE-24 and SE-17 suggest that the two are mutually discontinuous, with a fault located in the vicinity of El Marullero river.	SE-23 and SE-24 are located in a zone of low residual gravity anomaly

Section	Apparent resistivity	Projected ground structure	Comments
2. From the middle of SE-7 - SE-9 to the E1 Marullero river	Shallow layers: 200 Ω m Deeper layers: 2-40 Ω m	Pyroclastic materials are estimated as distributed to considerable depth throughout this section. On the basis of apparent resistivity values, pyroclastic materials are considered saturated from 100 m depth with groundwater from surface. Judging from apparent resistivity values for SE-9 and SE-7, the two are discontinuous and presumed interceded by a fault	This section is considered located within a zone of low residual gravity anomoly.
3. Environs of SE-7	Shallow layers: 80 Ω m Deeper layers: 3,000 Ω m	Apparent resistivity values imply that shallow bed of pyroclastic materials is thin, underlain by rock with resistivity of 3,000 Ω m. As outcroppings of limestone are visible in the vicinity, the latter layer of high resistivity is considered to be either Tertiary andesitic lava or limestone. SE-1 and SE-2 are assumed to be mutually discontinuous, interceded by faulting, on the basis of apparent resistivity values.	

Section	Apparent resistivity	Projected ground structure	Comments
4. West of SE-1	Shallow layers: 200-380 Ω m	Basalt, welded tuff and limestone out-croppings are in evidence in the environs of SE-1.	
	Deeper layers: 19-63 Ω m	Results from No. 1 and No. 2 borings indicate the layer of pyroclastic materials in this area is thin, whereas welded tuff basalt and limestone is present from 200 m depth. Judging from low apparent resistivity values, these layers are assumed saturated with groundwater.	

(2) B-B' Profile (see FIG. VI-7)

This profile stretches from west (Lo de Batres) to east (Finca Campo Nuevo).

Analysis of this profile is as below.

Section	Apparent resistivity	Projected ground structure	Comments
1. West of Cavelitos river	Shallow layers to 200 m depth: 400 Ω m	Based on apparent resistivity values, west of Cavalitos river is concluded as composed of pyroclastic materials.	This section is situated in a zone of steady increase from low to high residual gravity anomaly.
	Deeper layers: 50-90 Ω m	This layer is assumed to extend to considerable depth. The layer from ground surface to 200 m depth is considered, due to high apparent	

Section	Apparent resistivity	Projected ground structure	Comments
		resistivity, to be composed of surface sedimentation, probably consolidated volcanic ash.	
2. East of Canalitos river	From ground surface to 200 m depth: 100-250 Ω m Deeper layers: 2-70 Ω m	East of Canlitos river is considered composed of thin layer of pyroclastic materials underlain by welded tuff. In the vicinity of SE-43, outcroppings of Tertiary andesite and besalt are seen.	
Overall, the profile evidences similar apparent resistivity below a depth of 200 m, regarding which said layer is considered saturated.			

(3) C-C' Profile (see FIG. VI-8)

This profile stretches from north (Los El Presales) to south (Del Maestro).

Analysis of this profile is as below.

Section	Apparent resistivity	Projected ground structure	Comments
1. Entire profile	Shallow layers: 100-380 Ω m Deeper layers: 2-50 Ω m	The profile testing line runs along a north-south fault line presumed from aerial photographs. On the basis of apparent resistivity, the area is considered composed of pyroclastic materials. This layer	SE-17 and SE-47 are located at the eastern extreme of a zone of low residual gravity anomaly.

Section	Apparent resistivity	Projected ground structure	Comments
		is thick, extending to considerable depth. A saturated zone constituting a good aquifer is assumed below 100 m depth.	

(4) D-D' Profile (see FIG. VI-9)

This profile stretches from north (Finca la Dumbre) to south (Finca Monitas).

Analysis of this profile is as below.

Section	Apparent resistivity	Projected ground structure	Comments
1. North of SE-10 vicinity	Shallow layers: 100-500 Ω m Deeper layers: 200-220 Ω m	Shallow layers are considered composed of pyroclastic materials. Judging from surface geology near test sites, deeper layers consist of graywacke or lava basement. Geologic structure is complex.	
2. Vicinity of SE-8, SE-7	Shallow layers: 6-85 Ω m Deeper layers: 3000-3500 Ω m	Shallow layer of pyroclastic materials is considered very thin. Below this layer, on the basis of apparent resistivity and surface geology in the vicinity, there is a possibility of limestone presence. Conparison of SE-10 and SE-5 apparent resistivity values indicates discontinuity of resistivity	

Section	Apparent resistivity	Projected ground structure	Comments
		values between SE-8 and SE-7, with accordant assumed presence of faulting.	
3. South from Canalitos to No. 2 boring site	From ground surface to 200-300 m: 50-190 Ω m Deeper layers: 2-70 Ω m	Surface layer of pyroclastic materials is considered thick, underlain by welded tuff and basaltic sediments.	

(5) E-E' Profile (see FIG. VI-10)

This profile stretches from north (Finca Gracias Dios) to south (Los Ocotes).

Analysis of this profile is as below.

Section	Apparent resistivity	Projected ground structure	Comments
1. North of SE-13 vicinity	From surface to 200-400 m depth: 50 Ω m Deeper layers: 600-650 Ω m	Apparent resistivity of surface layer is low. Surface geology in the vicinity of the profile line implies the presence of pyroclastic materials distributed over a wide area. Underlying this is considered to be andesitic and basaltic rocks which feature high resistivity values.	

	Section	Apparent resistivity	Projected ground structure	Comments
2.	Vicinity of SE-11	Shallow layers: <100 Ω m Deeper layers: 3000 Ω m	Judging from apparent resistivities for SE-8, SE-7 and SE-11, the presence of limestone is considered possible.	
3.	South of SE-4 vicinity	Shallow layers: 250-1100 Ω m Deeper layers: 10-70 Ω m	Apparent resistivity of surface layer is extremely high. Welded tuff, lava and basaltic rock are distributed at the surface, and judging from apparent resistivity values, this layer is considered dry. Underlying layer is concluded to be the same type of rock, however it is assumed to be saturated.	

(6) <u>H-H' Profile</u> (see FIG. VI-11)

This profile stretches from Southwest (Vista Hebmos) to Northeast (Canalitos).

Analysis of this profile is as below.

Section	Apparent resistivity	Projected ground structure	Comments
Entire profile	From surface to depth of 50-300 m: 100-3000 Ω m Deeper layers: 2-70 Ω m	Apparent resistivity values between SE-32 - SE-36 exhibit a wide range of variance from 300 - 3,000 m. This condition extends to 300 m below the sûrface. Judging from surface geology, this layer is generally assumed	

(7) <u>I-I' Profile</u> (see Fig. VI-12)

Apparent resistivity of SE-31 is a somewhat high 190 Ω m from the surface to a depth of approximately 300 m. As with B-B' profile, this is considered due to a certain degree of subaerial sedimentation of well compacted volcanic ash. Below this layer, apparent resistivity is low at 27 Ω m. Judging from surface geology, this underlayer is assumed to be welded tuff in sturateed sate.

(8) <u>J-J' Profile</u> (see Fig. VI-13)

Apparent resistivity in and around SE-22 and SE-32 in the 180-295 Ω m range from the surface to a depth of 200-300 m. As with I-I' profile, this is considered to indicate subaerial sedimentation.

Below this is material of low appararent resistivity assumed to be welded tuff in saturated state.

Section	Apparent resistivity	Projected ground structure	Comments
		to be pyroclastic materials. The layer extends to considerable depth between SE-31 - SE-26. Deep layer of low resistivity is considered to be welded tuff in saturated state.	

(9) F-F' Profile (see FIG. VI-14)

Analysis of this profile is as below.

	Section	Apparent resistivity	Projected ground structure	Comments
1.	Vicinity of SE-55	200-14,000 Ω m	Uplifting of basement rock close to surface is assumed.	High residual gravity anomaly is present.
2.	From Molino river to La Barranca river	Shallow layers: 400-500 Ω m Deeper layers: 70 Ω m	Pyroclastic materials are deposited to considerable depth. Deeper layers are considered as probably limestone.	Low residual gravity anomaly is present.
3.	From Zapote river to Molino river	Shallow layers: 300-500 Ω m Deeper layers: 150-300 Ω m	Compared with 2 above, pyroclastic materials layer is thinner. This is considered underlain by limestone and granite.	Possibility exists for transition from low to high residual gravity anomaly through the zone.
4.	North of Zapote river	Shallow layers: 60 Ω m Deeper layers: 250-400 Ω m	As granite outcroppings are present on the surface, pyroclastic materials layer is concluded as thin.	

(10) G-G' Profile (see FIG. VI-15)

Analysis of this profile is as below.

	Section	Apparent resistivity	Projected ground structure	Comments
1.	East of Marullero river	330 Ω m	Limestone outcroppings are present on the surface. Limestone in vicinity of SE-51 slopes sharply at 70° with dip orientation to the east.	Residual gravity anomaly is +
2.	From Marullero river to Q. Pansiguir river	Shallow layers: 500 Ω m Deeper layers: 200 Ω m	Pyroclastic materials layer in SE53 - SE-61 is thick. Underlying layer is possibly limestone.	Residual gravity anomaly ranges from + to -
3.	West of Q. Pansiguir river	Shallow layers: 60 Ω m Deeper layers: 200-400 Ω m	Presence of limestone outcroppings in the east indicate steadily decreasing thickness of pyroclastic materials layer in that direction. Underlying layer is considered to be limestone and granite.	Residual gravity anomaly ranges from - to +

6.2.6 Considerations on Results of Electrical Prospecting

The following is a description of the results of electrical prospecting and the investigation performed for its relationship to the hydraulic geology structures of the eastern and northern (Cerro el Naranjo vicinity) sectors.

(1) Eastern Sector

In terms of geological structure, the eastern sector is an uplifted zone bounded by two north-south faults. However, there is the possibility that an east-west fault develops along national highway 9 to form a saddle-shape. Owing to this, the flow patterns of the free aquifer groundwater in this region are thought to consist of i) those that are recharged from the plateau near Puerta parada to the south, and that flow to the north, ii) those that are recharged by the highlands to the west, and that flow to the east of the east-west saddle-shape, and iii) those that are partially recharged from the high land to the north, and that meet to flow north-east along national highway 9.

Three planar distribution maps (EL 1400 m, EL 1300 m and EL 1200 m) were complied from the results of VES curve analysis and indicated no large difference in the apparent resistivity distributions for each level. The correspondence between the type of rock structure and the apparent resistivity values for this area are shown in TABLE VI-4. The following is a brief description of these relationship.

- o The 50 Ω m or less range corresponds to Pyroclastic material or tuff while there is the possibility that it may also be saturated by groundwater.
- o The 100 Ω m or more range corresponds to Welded tuff or Andesite Basalt lava, while the 1000 Ω m or more range is thought to correspond to limestone or Basalt (Cretaceous).

Fig. VI-16 (1) (2) show the apparent resistivity distribution diagram and the groundwater depth distribution diagram for EL 1200 m of this region. According to these figures, there is an extermely good correspondence between the low resistivity band

(50 to 100 m) and the groundwater level distribution conditions at depths of below 100 m. This suggests the relatively thick sedimentation of Quarternary tuff and Pyroclastic with a high ratio of gaps for this range, and therefore the high possibility of the existence of free aquifer at depths below 100 m.

On the other hand in the high resistivity band thought to correspond to coal shale and basalt, the water level of the unconfined groundwater is generally about 70 m below the surface (and thought to be directly above the basement) and has an extremely small pump-up volume. This is thought to suggest that the basement is located at a shallow depth and that in regions of sloping ground, the groundwater flows down to follow the slope and therefore has a small storage volume. Accordingly, either the central portion of the sedimentary basin or the troughs forming the arteries should be the object in order to obtain a free aquifer of large volume. For Test Well #2 (of depth 300 m) implemented as part of this survey, there were Pyroclastics to a depth of 240 m and Andesite below that, with the water level being at approximately 95 m. Because of this, it is thought that an free aquifer exists in a saturated state between the depths of 95 m and 240 m. A pump-up test was performed for the Andesite, with there being practically no lowering of the water level when water was pumped at 50 l/sec. This is interpreted as indicating that water was being pumped-up from the lower aquifer, and not from the free aquifer.

At the Project 3-4 bores in the northern block and the Ojo de Agua sector in the southern sector, the presence of a lower aquifer in the basement was confirmed at EL 1300 m, leading to the expectation of a lower aquifer for below 1300 m in this region. However, in Test Wells No. 1 and No. 3, despite the groundwater levels in the basement being 1300 m and 1213 m respectively, the pump-up volume was extremely small at 5-6 l/sec for both. For both places, this indicates the possibility of there being a hard basement with little cracking, and therefore necessitating the implementation of a detailed geological survey to determine the range for which the lower aquifer exists.

(2) Northern Sector (see Cerro el Naranjo)

When compared to the eastern sector, this sector has a relatively high value for the apparent resistance, with coal shale, Andesite and granite being recognized on the surface. The basement is therefore thought to exist at a relatively shallow depth. Nevertheless, because Guatemala city rests on a basin structure, few borings down to the basement have been performed for this sector but the average pump-up potential has been estimated to be 11-14 l/sec for groundwater levels at depths of 30 m - 100 m, with the greater part thought to be free aquifer.

The deep well in this sector was the Proyect 4-3 bore (EL 1467 m, 304 m deep) in the north. For this bore, there was basement coal shale at a depth of 115 m, with the groundwater level being 167 m (EL 1300 m) and the pump-up volume being very large at 63 l/sec.

The water level is in conformity with the artesian flowing well level for the Ojo de Agua block in the southern sector, and extremely similar to the water level of the Test Wells #1 and #2 in the eastern sector.

This means that this groundwater is a lower aquifer, and that future test bores should be implemented with this lower aquifer as the object. However, the landform of this sector is high at EL 1500 m or more and so it is therefore desirable that the boring depth be increased or that borings be implemented in the lowland sector to the east in order to treat this lower aquifer as the object.

6.3 ELF - Magneto - Telluric Resistivity Method

The purpose of the subject survey is to identify the planar distribution of ground resistivity.

The magneto-telluric method attempts to determine distribution of ground resistivity through measurement of naturally existing magnetic and electrical fields.

The electromagnetic mapping method applied in the subject survey utilizes from among the ELF (extremely low frequency, 1-3,000 Hz) band of natural electromagnetic waves, the particularly intense Shoeman resonance frequencies (approximately 8, 14, 20 Hz...).

The purpose of this survey is to clarify the planar distribution of the apparent resistivity of the ground, as a supplement to the Schlumberger survey described in 6.2. In general, the measurement depths corresponding to the apparent resistivity distribution are shown below for the skin depth ($\delta = 0.503 \times \sqrt{\rho/f}$ km).

Apparent resistivity is distributed in a range of 2-500 Ω m for the 3 types of apparent resitivity distribution maps (8 Hz, 14 Hz and 20 Hz) were obtained (see FIG. V-17).

Apparent Resistivity	8 Hz	14 Hz	20 Hz
5 Ω m	400 m	300 m	250 m
50 Ω m	1,260 m	950 m	790 m
100 Ω m	1,780 m	1,340 m	1,120 m
500 Ω m	3,980 m	3,000 m	2,490 m

Comparison of the 3 types of apparent resistivity distribution maps reveals a similar distribution for each Hz value. It is generally accepted that locations of low apparent resistivity tend to be high in water content. Well packed materials (for example, limestone with limited cracking, lava, welded tuff, etc.) have comparatively high apparent resistivity values. The surface geology within the Study area has a high apparent resistivity belt where deposits of welded tuff or andesitic-basaltic materials are believed present.

The extent of the high apparent resistivity belt decreasing in the following order of Hz values: 8 Hz → 20 Hz → 14 Hz. Apparent resistivity values increase as Hz values decline: 20 Hz → 14 Hz → 8 Hz.

For 20 Hz, a high water bearing/low apparent resistivity belt is distributed along national highway 9. This section is accordingly considered promising for development. These findings correlate with those of the groundwater flow direction survey and resistivity prospecting.

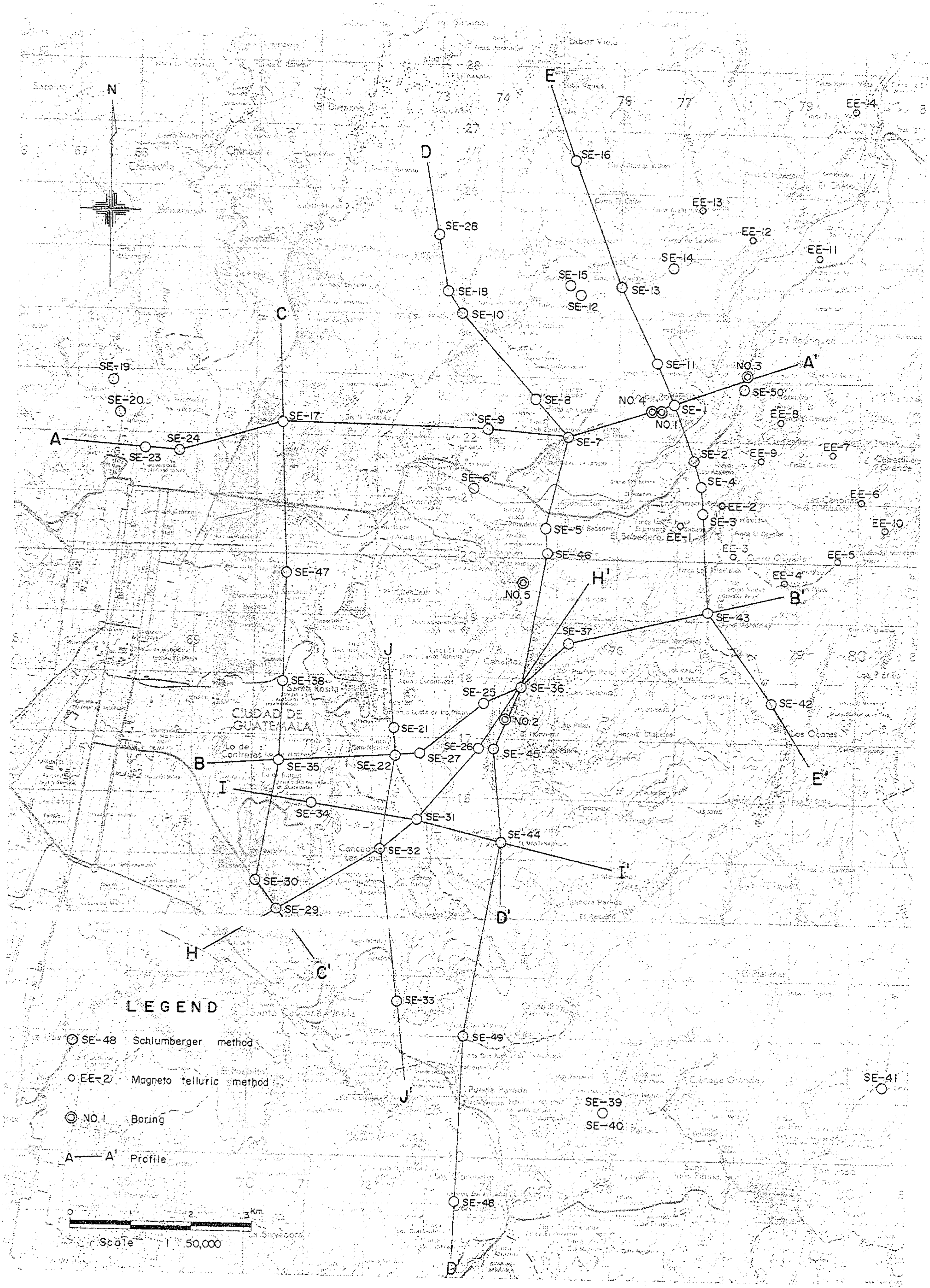

FIG. VI-4 SITE OF ELECTRICAL PROSPECTING

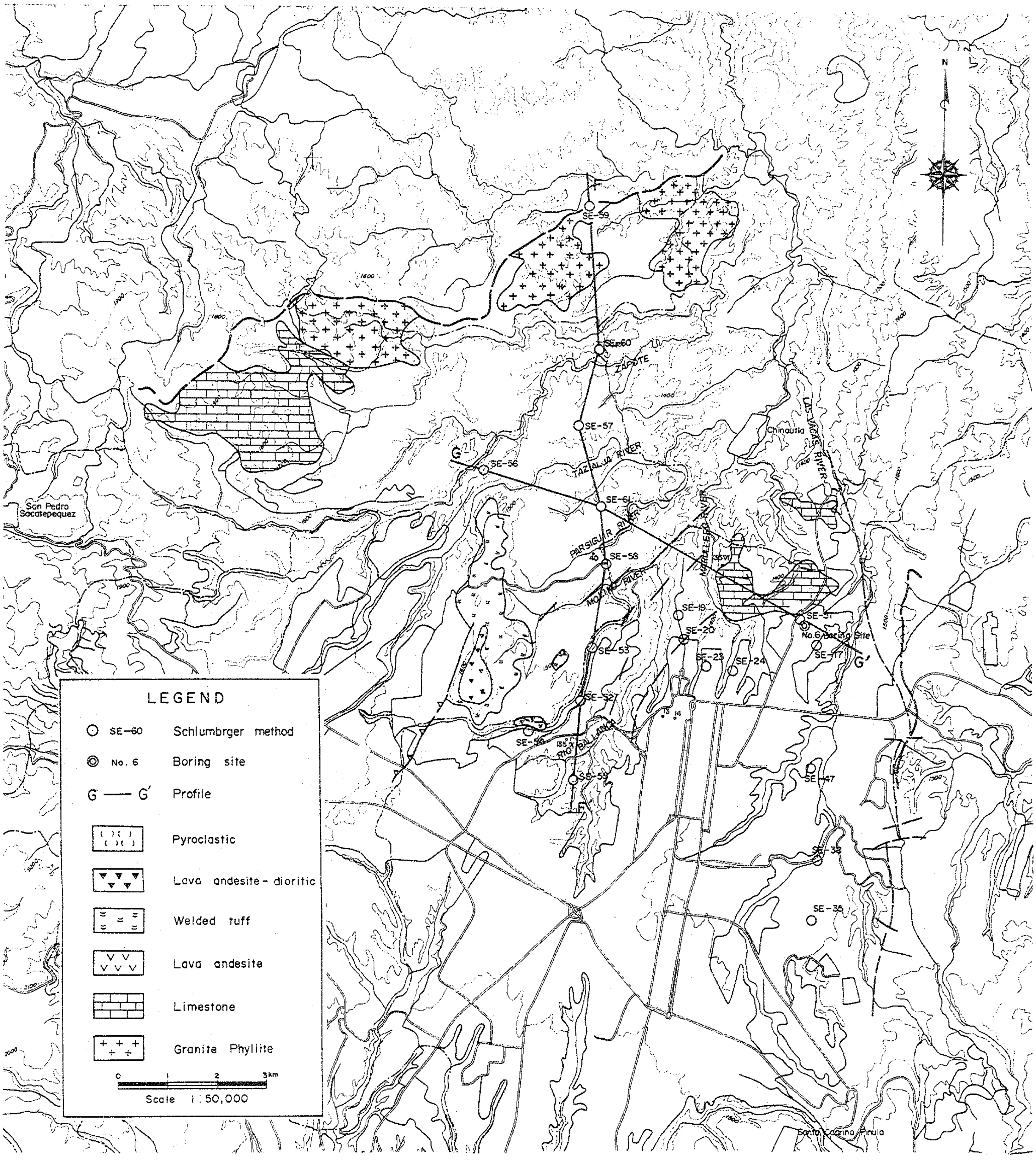

FIG. VI-5 SITE OF ELECTRICAL PROSPECTING
(NORTHERN AREA)

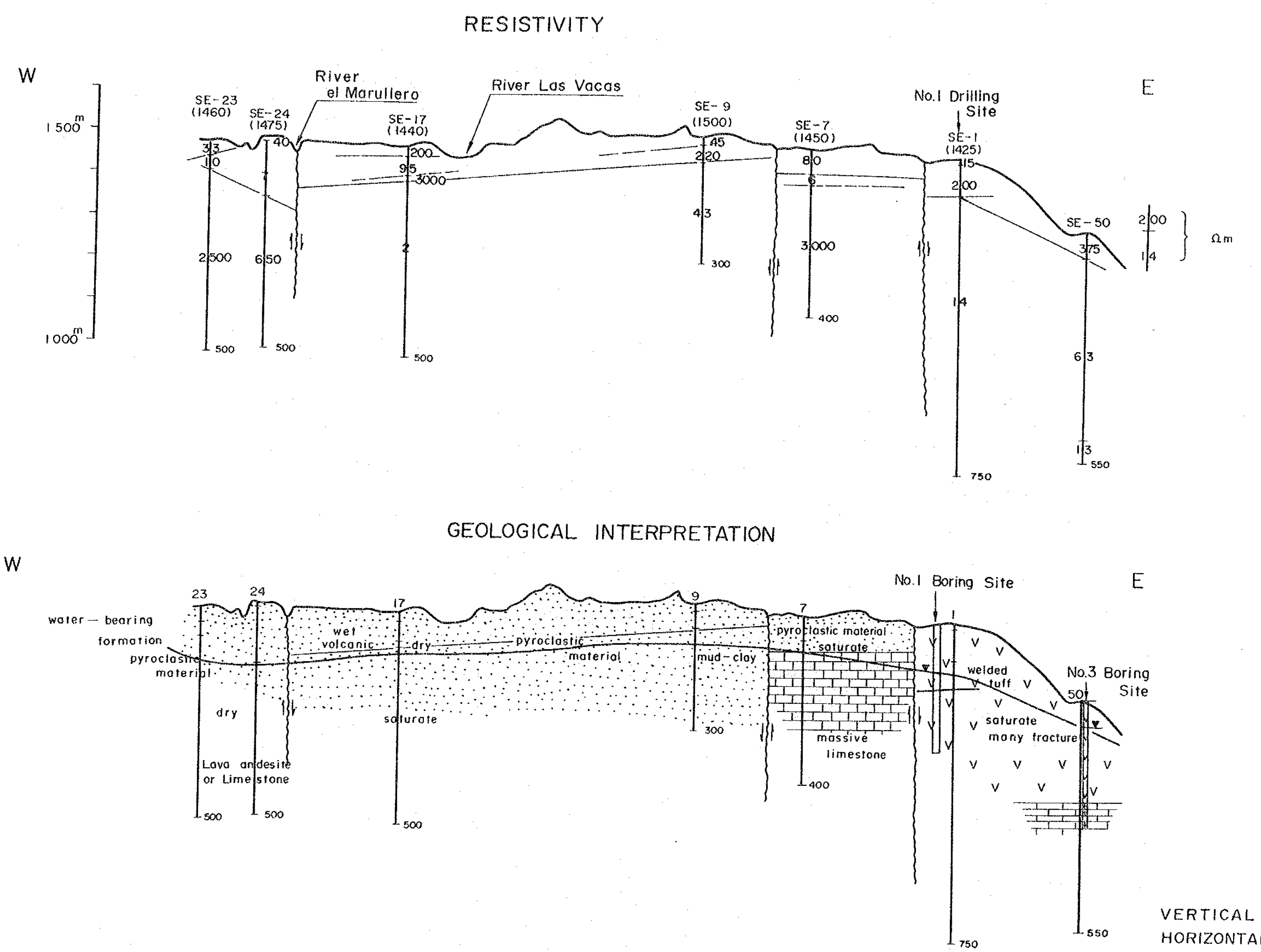

VERTICAL : 1 : 10,000
HORIZONTAL : 1 : 50,000

FIG. VI-6 A-A' PROFILE

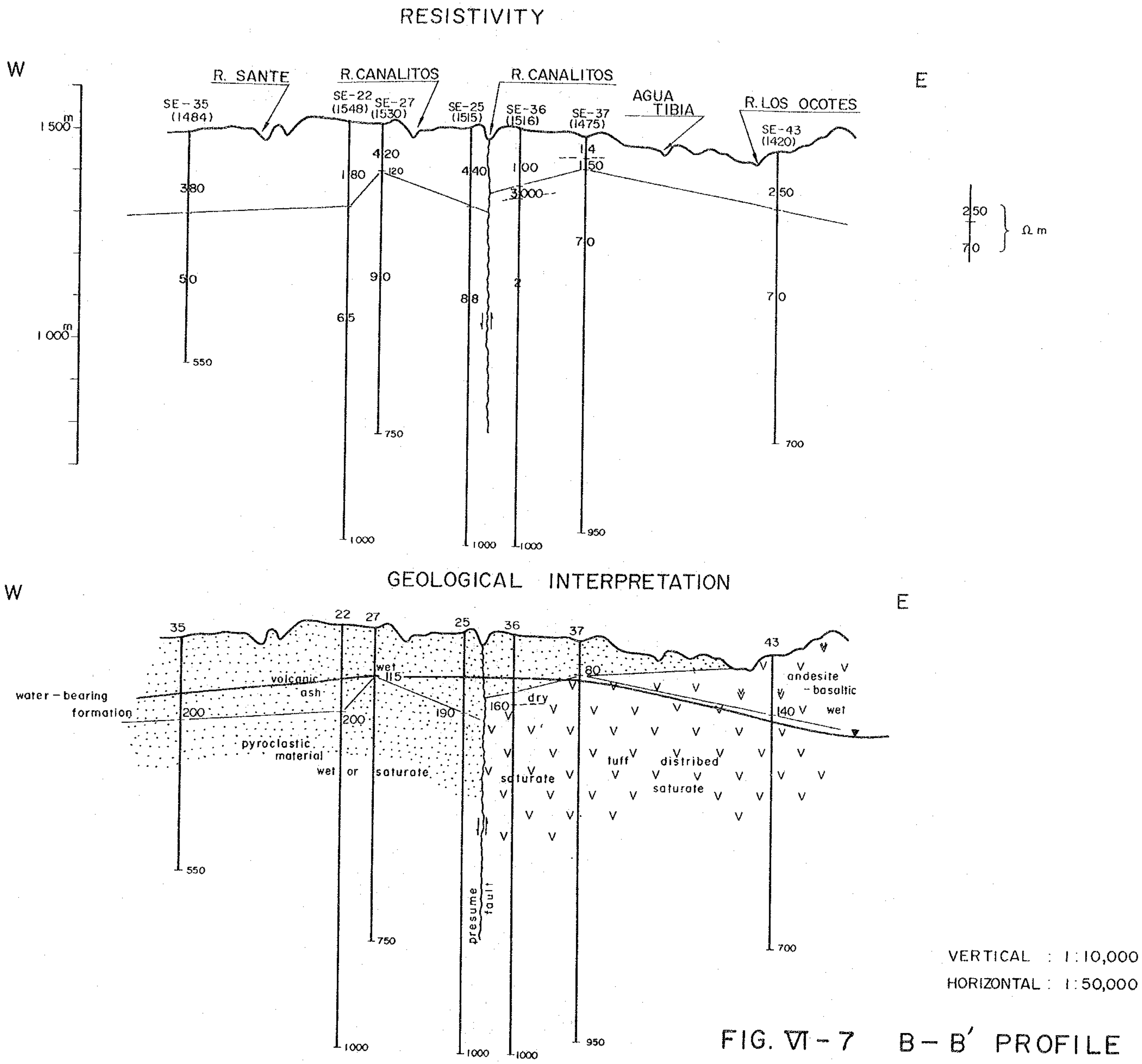

VERTICAL : 1:10,000
HORIZONTAL : 1:50,000

FIG. VI-7 B-B′ PROFILE

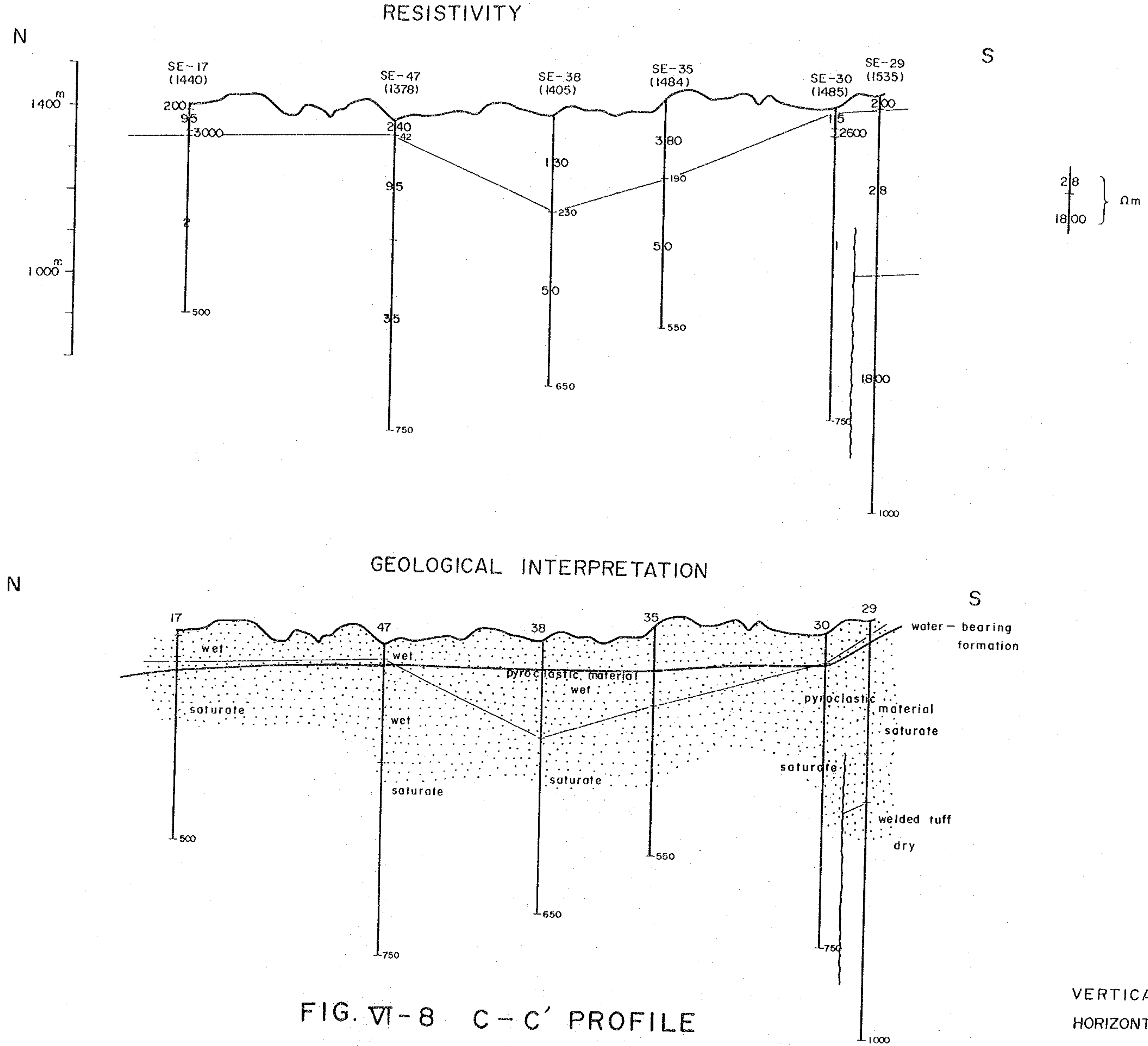

FIG. VI-8 C – C′ PROFILE

VERTICAL : 1 : 10,000
HORIZONTAL : 1 : 50,000

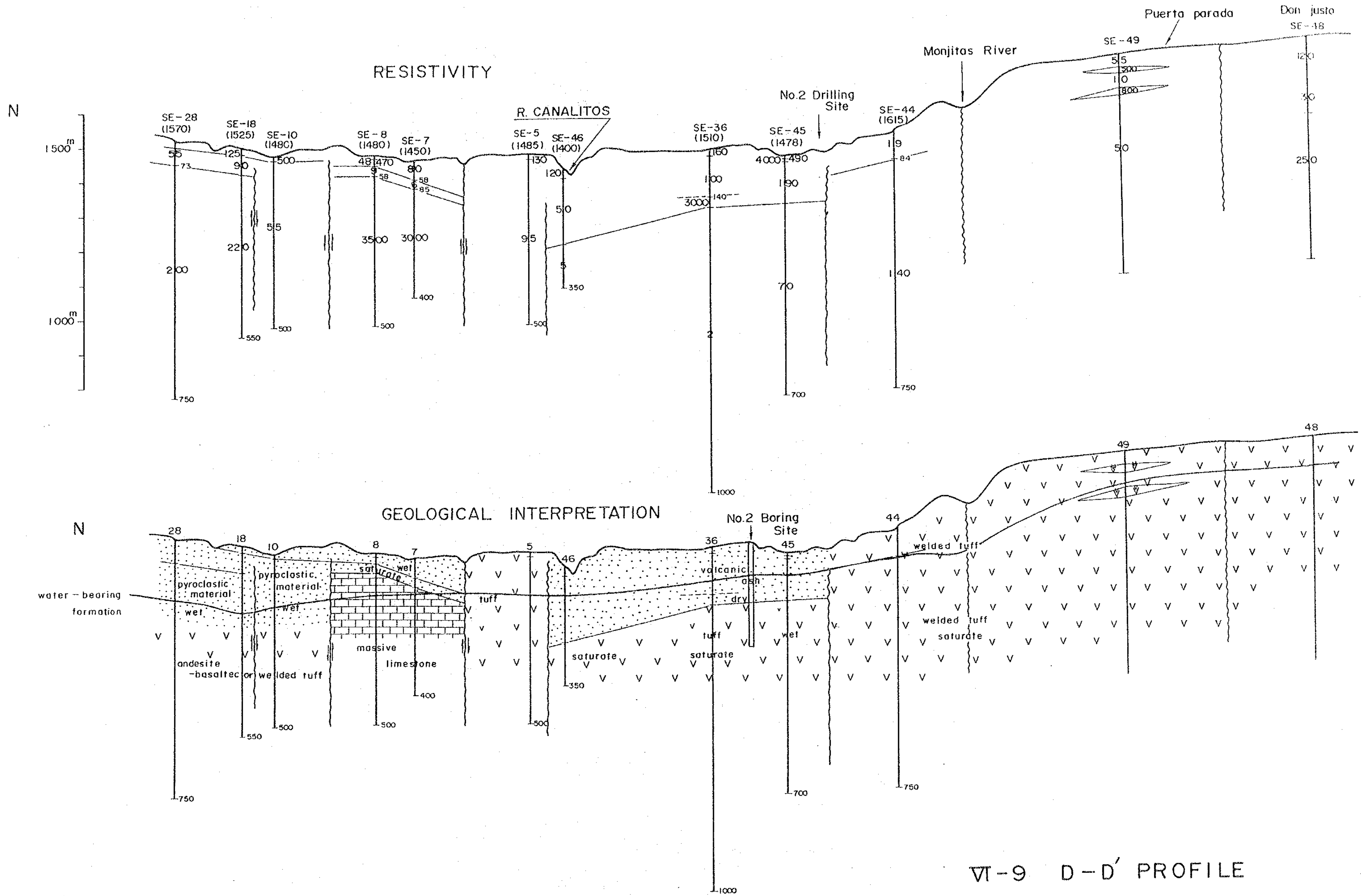

VI-9 D-D' PROFILE

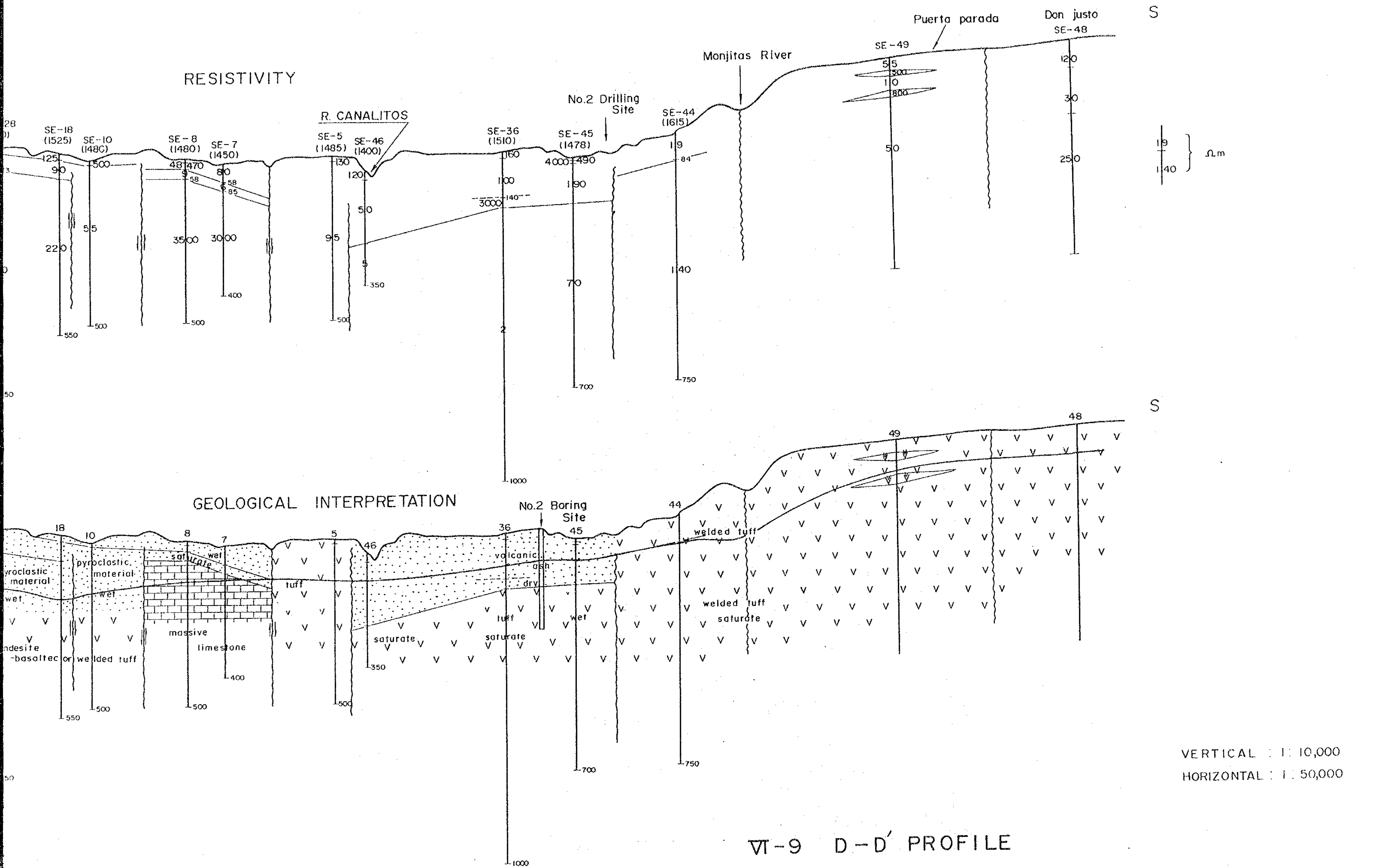

VERTICAL : 1 : 10,000
HORIZONTAL : 1 : 50,000

VI-9 D-D′ PROFILE

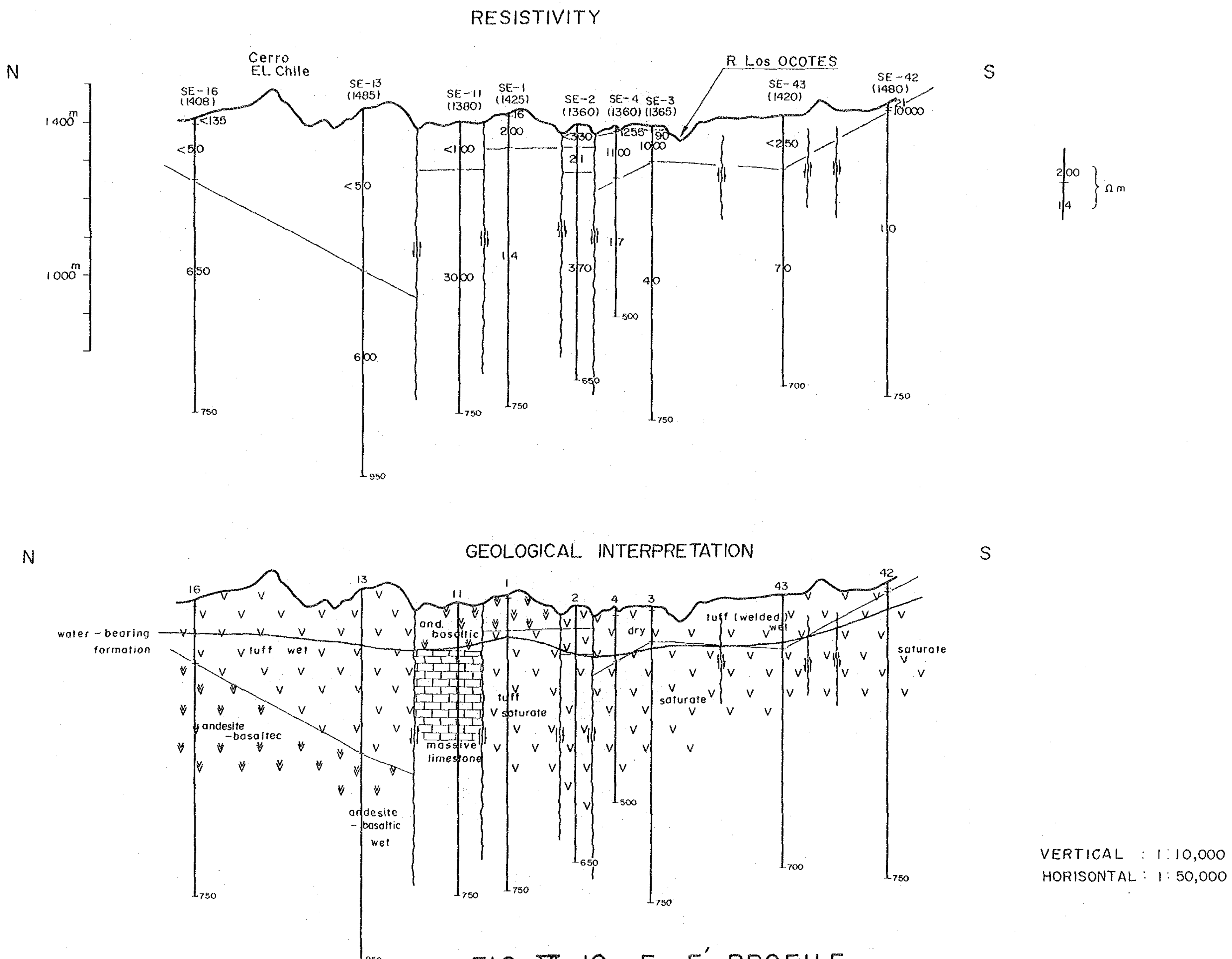

FIG. VI-10 E-E' PROFILE

RESISTIVTY

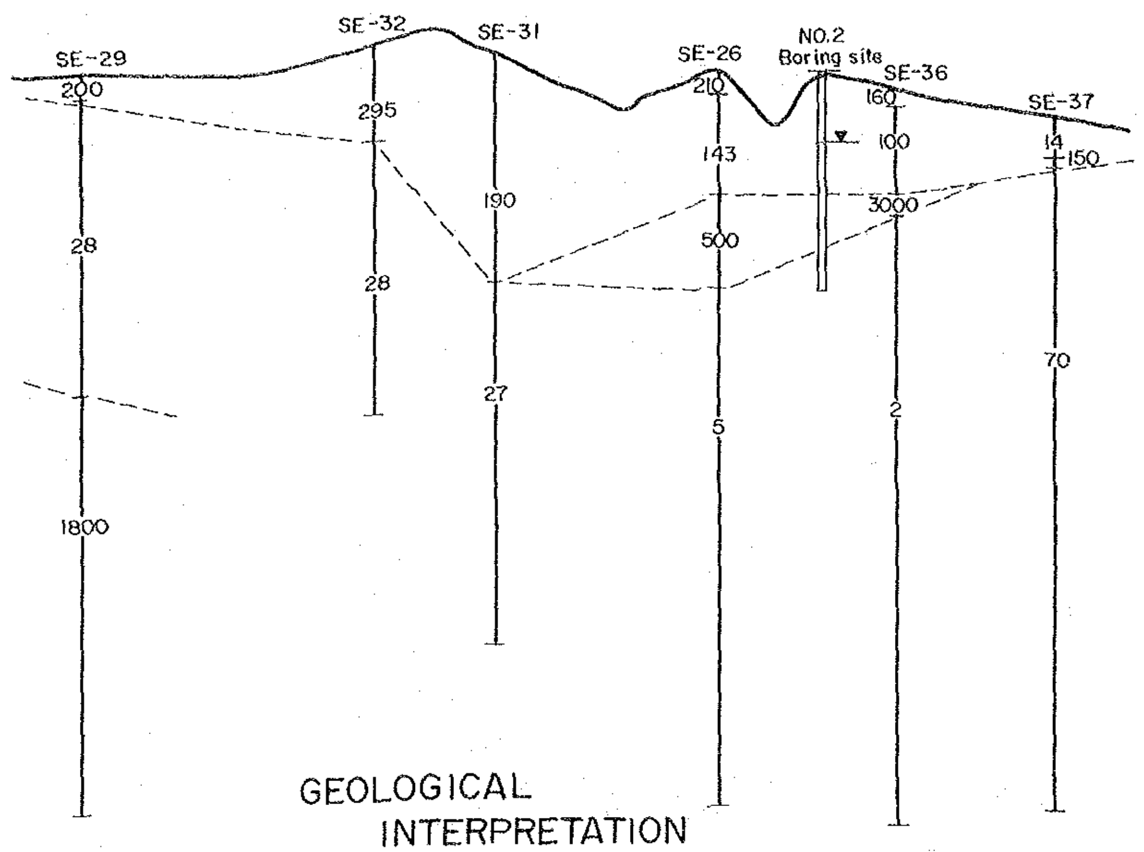

GEOLOGICAL
INTERPRETATION

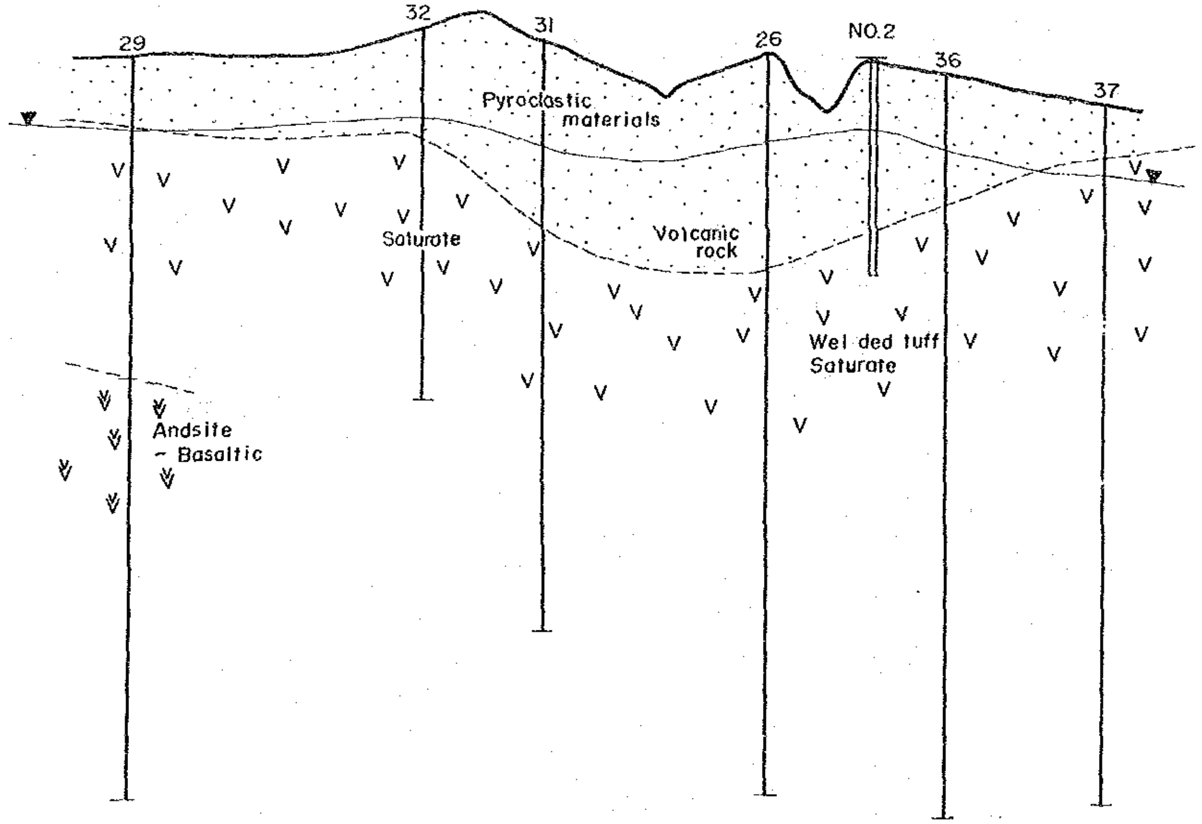

FIG. VI-11 H-H' PROFILE

VERTICAL 1 : 10,000
HORIZONTAL 1 : 50,000

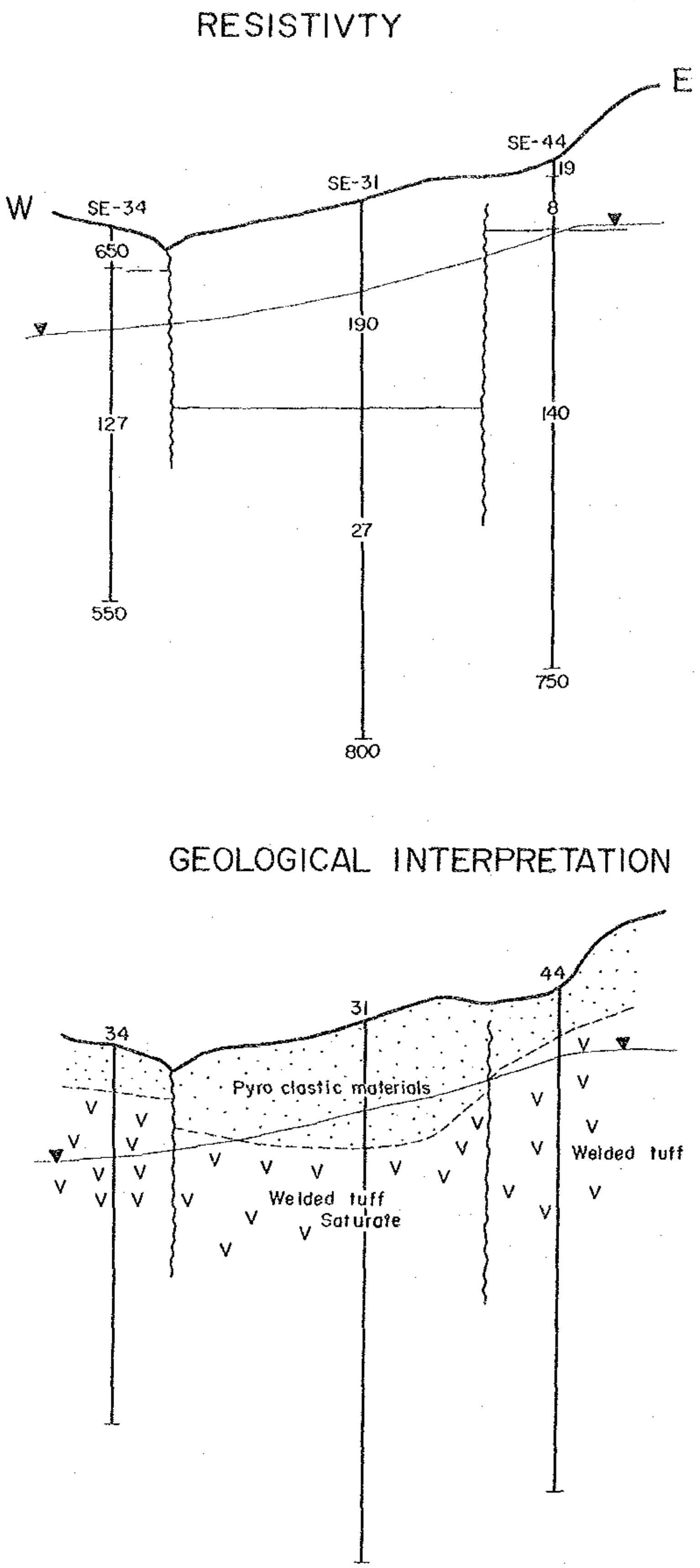

FIG. VI-12 I-I′ PROFILE

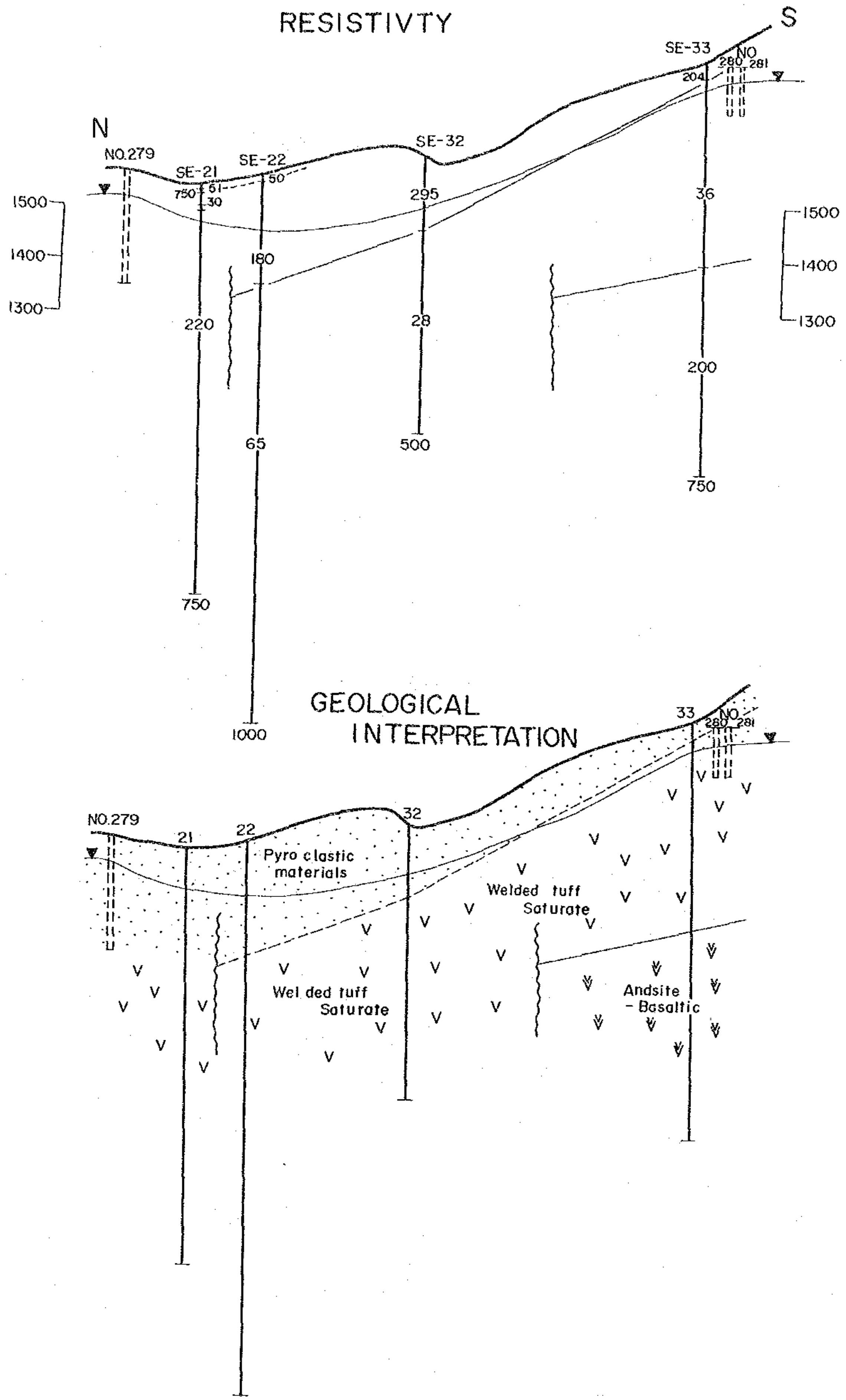

FIG. VI-13 J - J′ PROFILE

VERTICAL 1 : 10,000
HORIZONTAL 1 : 50,000

RESISTIVITY

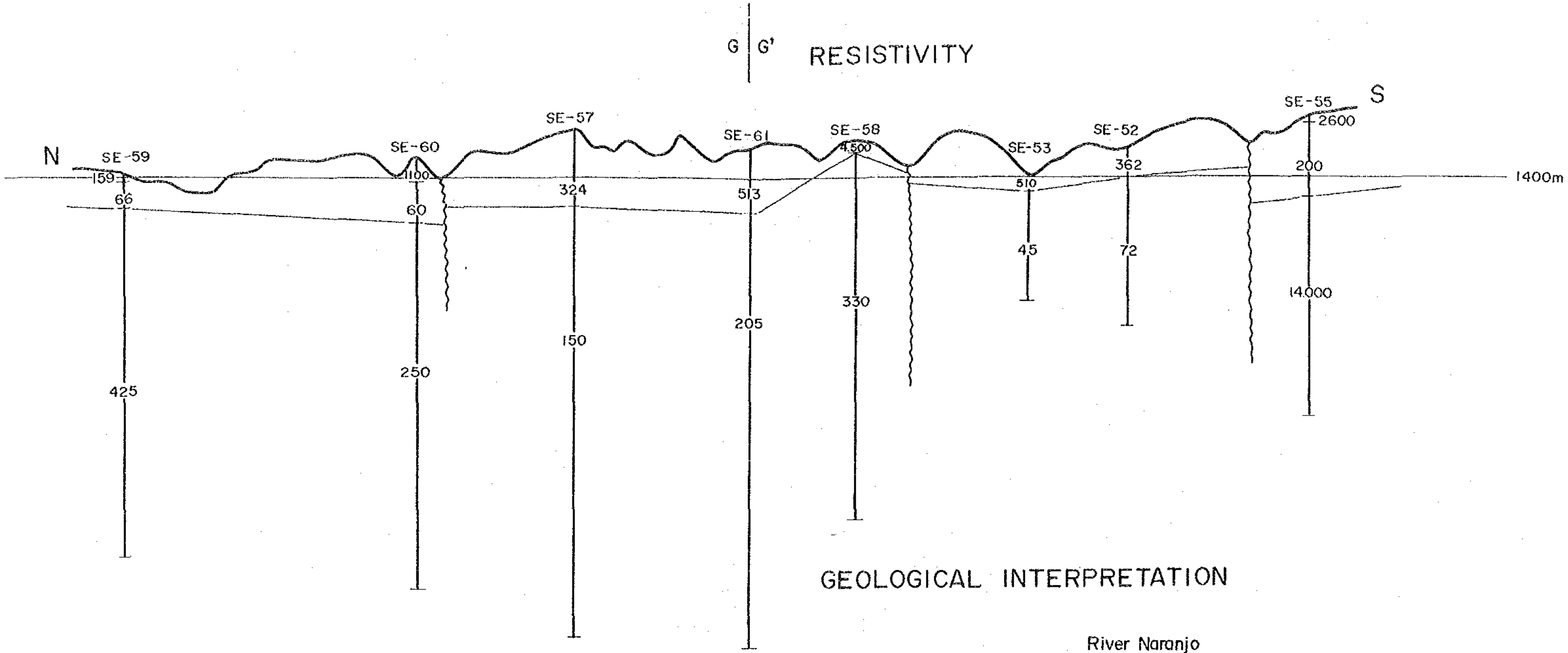

GEOLOGICAL INTERPRETATION

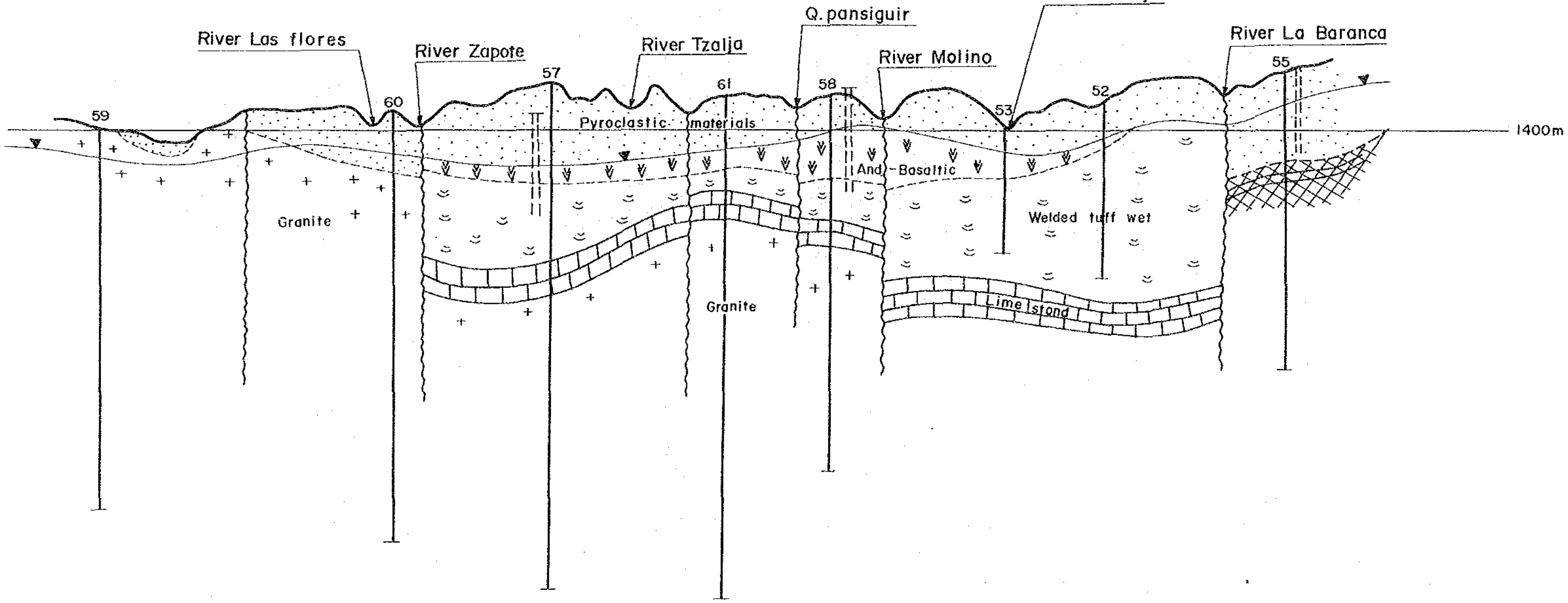

FIG. VI-14 F-F' PROFILE

VERTICAL 1 : 10,000
HORIZONTAL 1 : 50,000

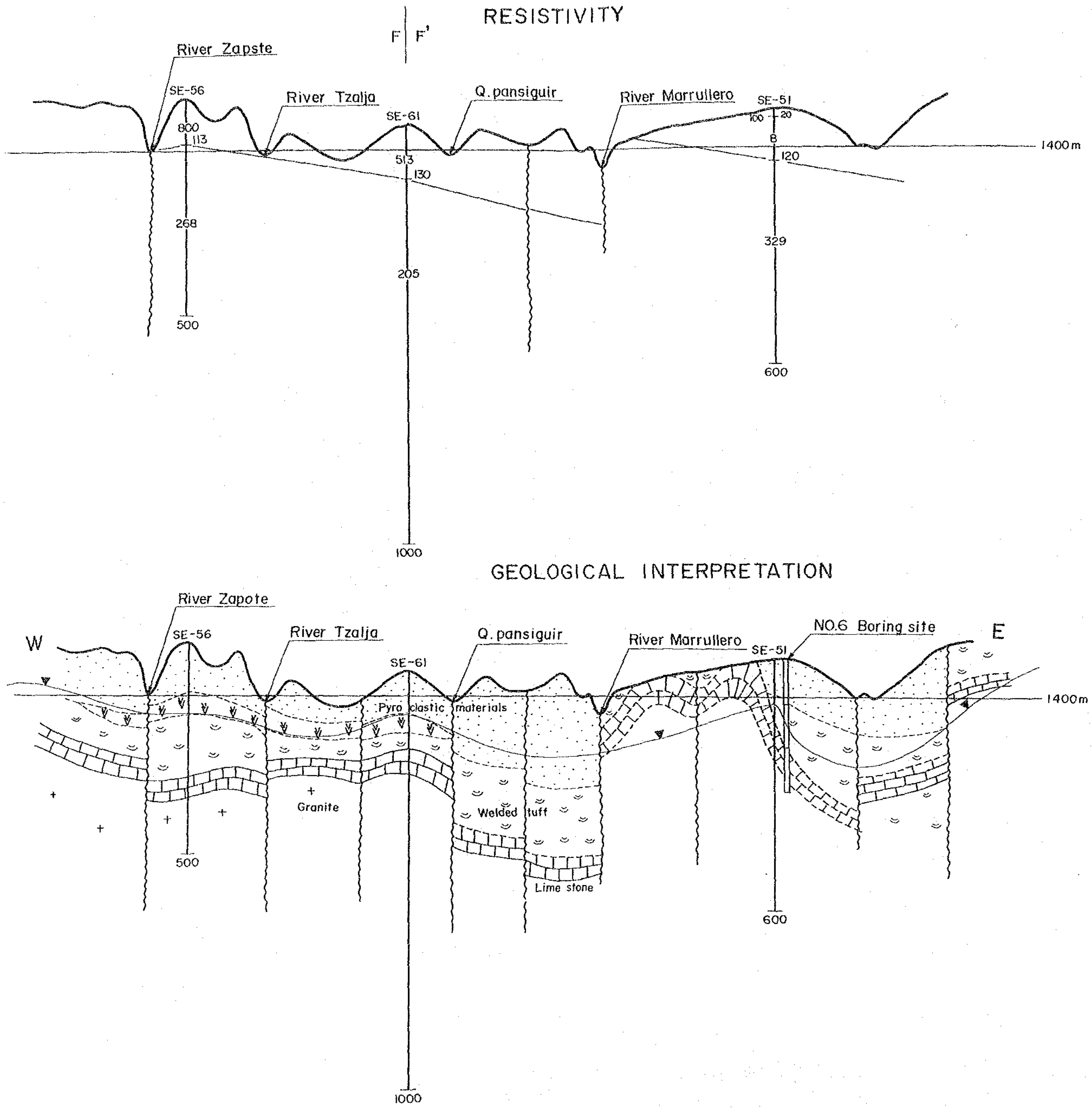

FIG. VI-15 G - G' PROFILE

VERTICAL 1 : 10,000
HORIZONTAL 1 : 50,000

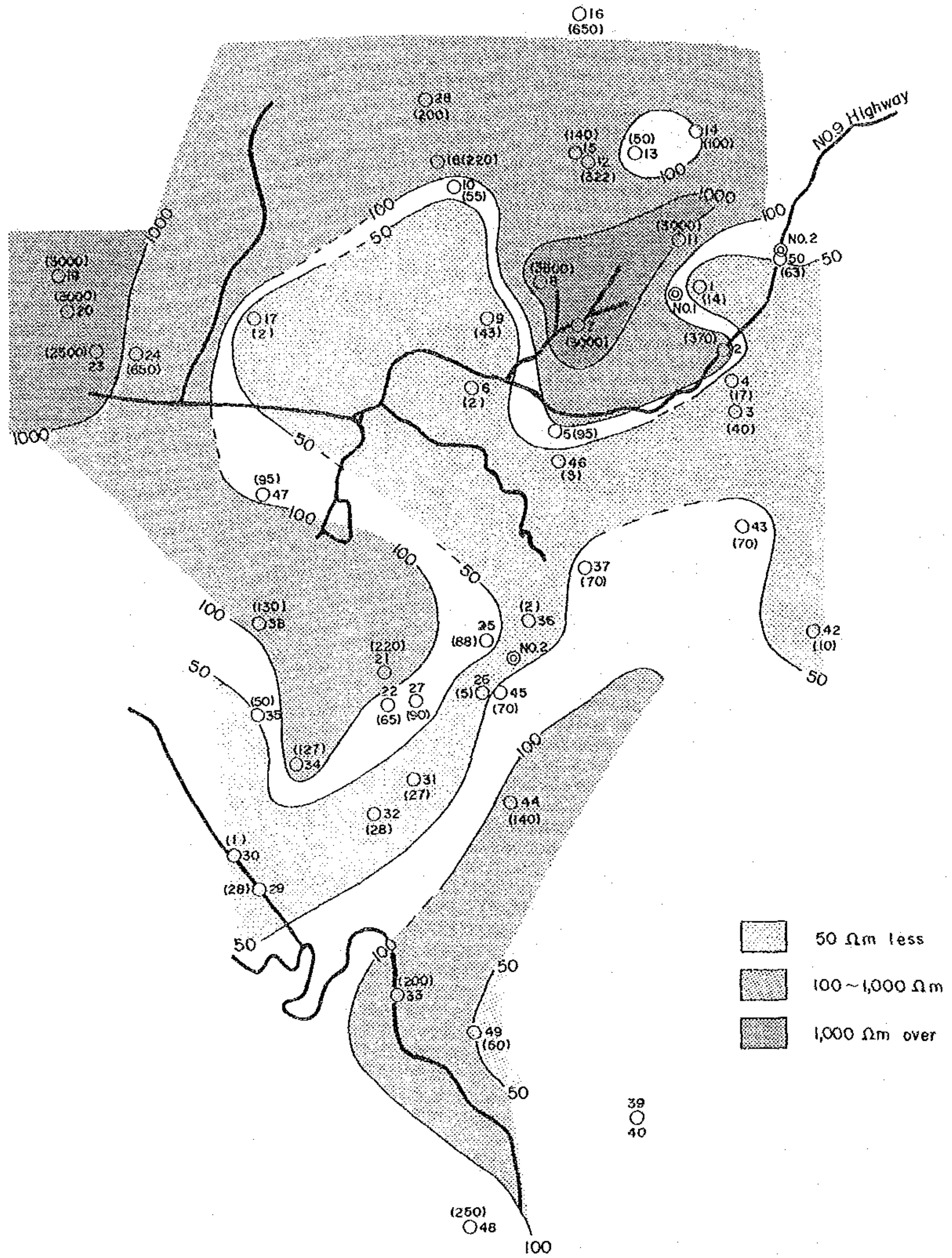

APPARENT RESISTIVITY (1)

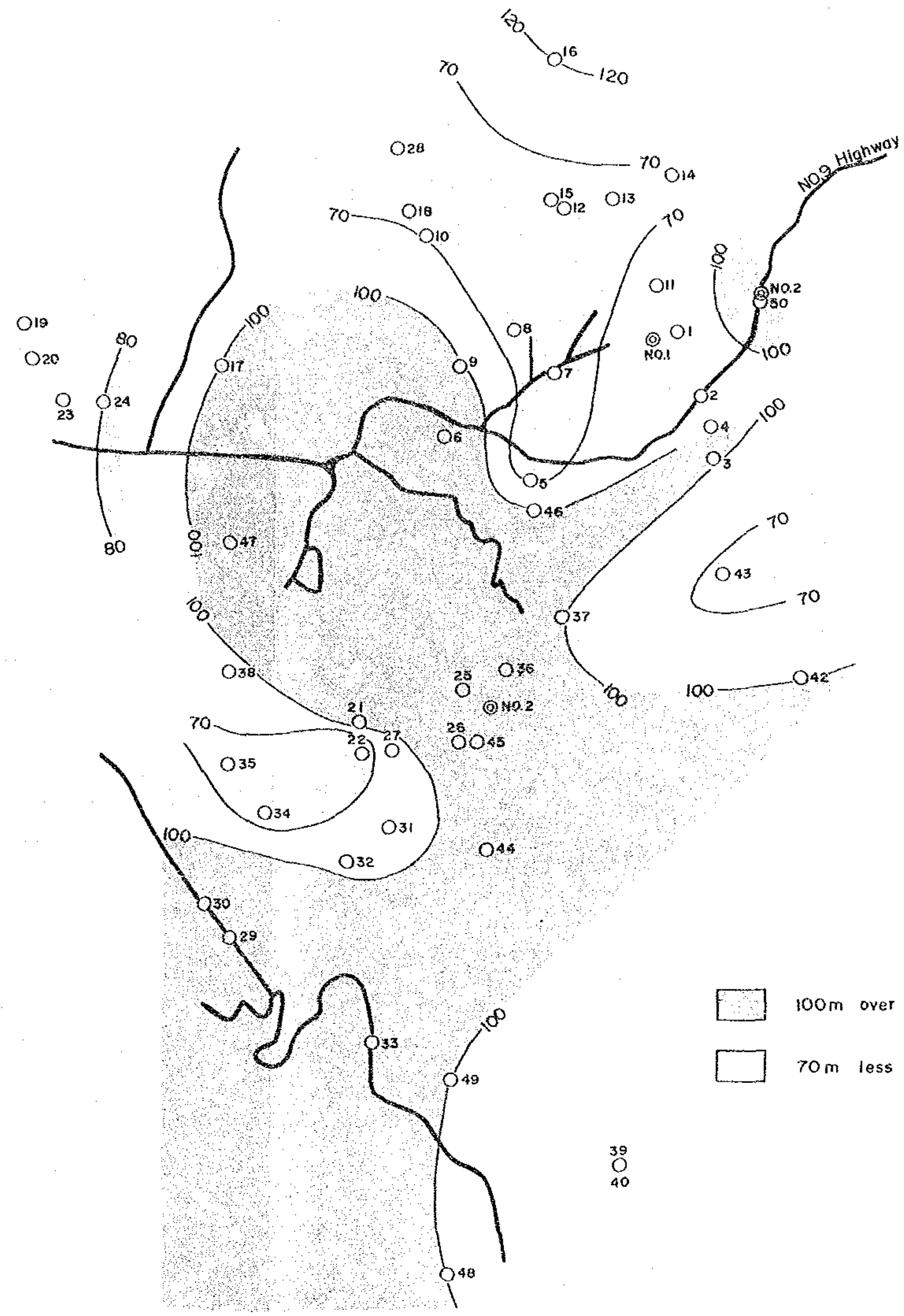

WATER TABLE (2)

FIG. VI-16 DISTRIBUTION OF APPARENT RESISTIVITY AND WATER TABLE AT 1200m ABOVE SEA LEVEL

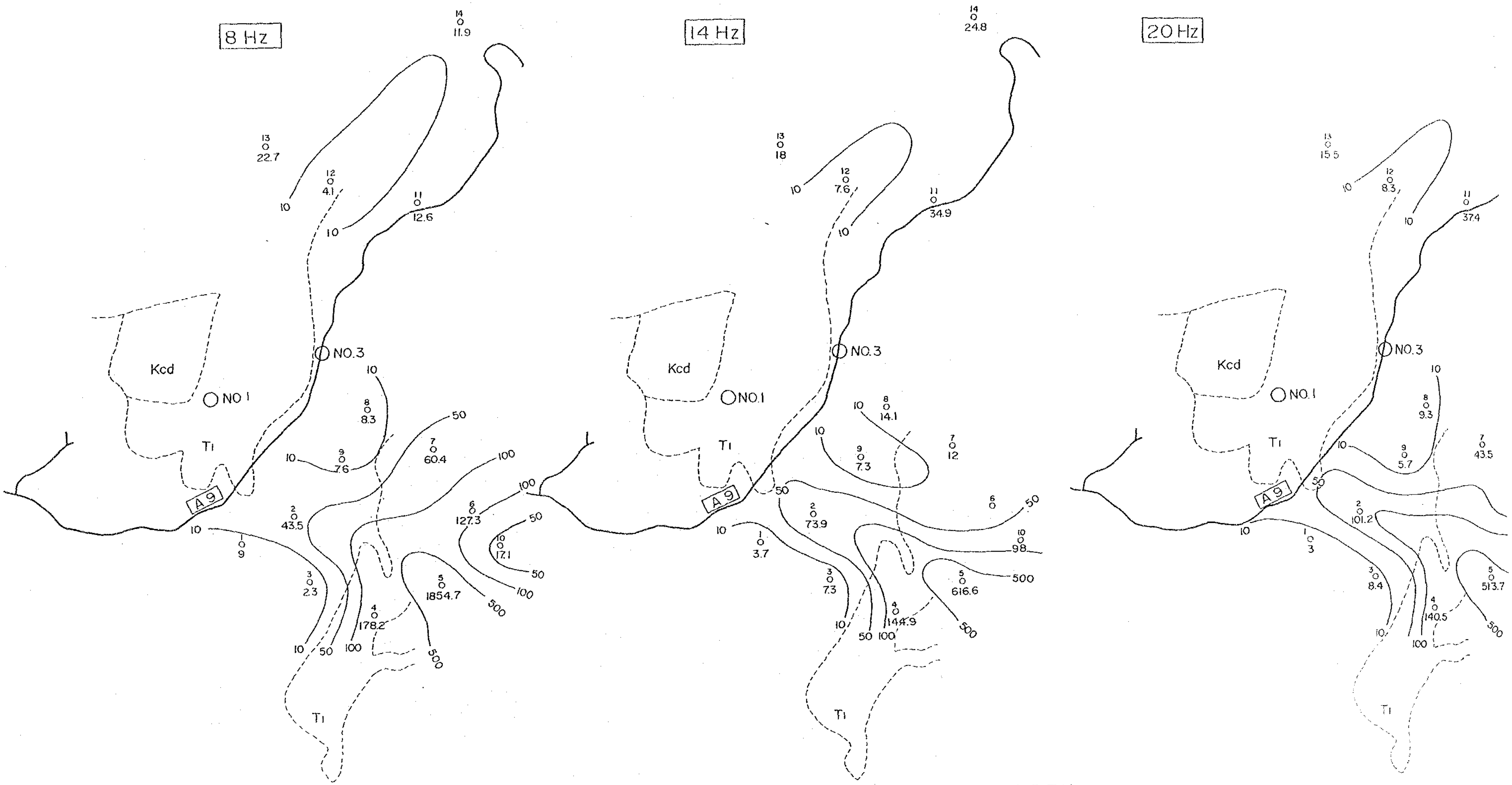

INDEX

- 8.3 — Mesurement point and Apparent resistivity
- 10 — Apparent resistivity (Horizontal)
- Locks distribution
- Boring site
- Kcd — Limestone and Dolomite
- T1 — Lava, Basaltic andsite

FIG. VI-17 CYCLE-WISE DISTRIBTION OF APPARENT RESISTIVITY

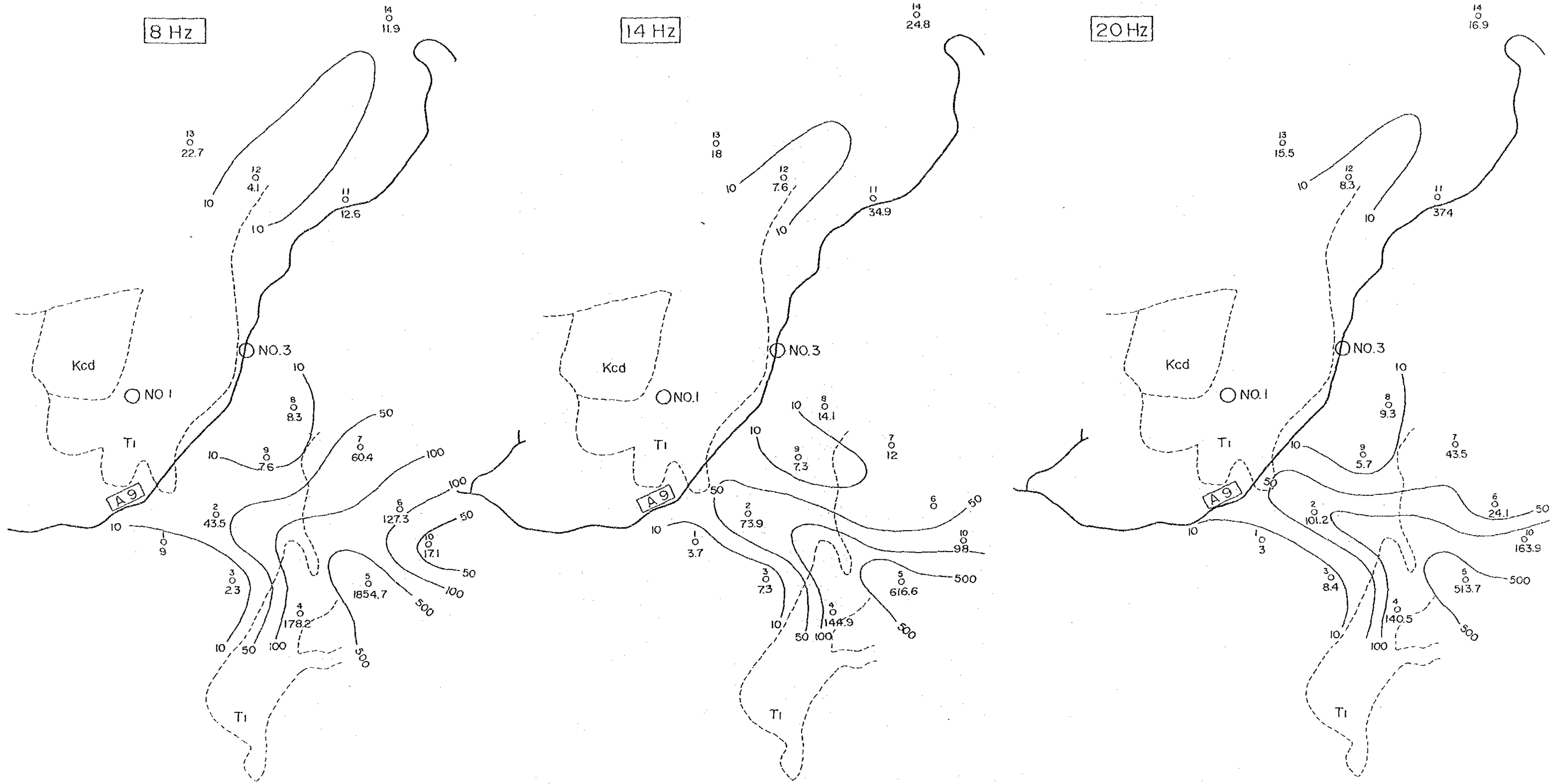

FIG. VI-17 CYCLE-WISE DISTRIBTION OF APPARENT RESISTIVITY

INDEX

- 8.3 — Mesurement point and Apparent resistivity
- 10 — Apparent resistivity (Horizontal)
- Locks distribution
- Boring site
- Kcd — Limestone and Dolomite
- T1 — Lava, Basaltic andsite

TABLE.VI - 2 ELECTRICAL SURVEY DATA SHEET

Area ____________________ Date ____________________

Line __________ Point Nº __________ Weather ____________________

Operator ____________________

L/2 (m)	1/2 (m)	V (mV)	I (mA)	K	a (-m)	Remarks
6	3			14.1		
10	3			47.6		
14	3			97.8		
18	3			165		
24	3			297		
30	3			467		
40	3			833		
50	3			1302		
60	3			1885		
80	3			3350		
	25			363		
100	3			5230		
	25			588		
130	25			1020		
170	25			1775		
	50			829		
200	25			2470		
	50			1178		
250	50			1885		
300	50			2750		
	100			1255		
400	50			4940		
	100			2360		
500	100			3770		
750	100			8680		
	250			3140		
1000	100			15550		
	250			5890		
1250	100			24400		
	250			9430		
1500	100			35200		
	250			13730		

****

TABLE VI-3 Data List Station No. E-25

****

No.	AB/2(m)	MN/2(m)	V(mV)	I(mA)	G.C.	A.R.(ohm%m)
(1)	6.0	3.0	5.10E+02	275	1.41E+01	26
(2)	10.0	3.0	1.97E+02	220	4.76E+01	43
(3)	14.0	3.0	1.28E+02	230	9.79E+01	54
(4)	18.0	3.0	8.89E+01	220	1.65E+02	67
(5)	24.0	3.0	6.41E+01	235	2.97E+02	81
(6)	30.0	3.0	4.30E+01	205	4.67E+02	98
(7)	40.0	3.0	2.89E+01	200	8.33E+02	120
(8)	50.0	3.0	4.65E+01	405	1.30E+03	150
(9)	60.0	3.0	3.83E+01	420	1.88E+03	171
(10)	80.0	3.0	2.54E+01	395	3.35E+03	216
(11)	80.0	25.0	2.02E+02	380	3.63E+02	192
(12)	100.0	3.0	1.97E+01	415	5.23E+03	248
(13)	100.0	25.0	1.58E+02	410	5.89E+02	227
(14)	130.0	25.0	1.01E+02	395	1.02E+03	260
(15)	170.0	25.0	5.51E+01	330	1.78E+03	296
(16)	170.0	50.0	1.07E+02	325	8.29E+02	272
(17)	200.0	25.0	5.80E+01	455	2.47E+03	315
(18)	200.0	50.0	1.13E+02	445	1.18E+03	299
(19)	250.0	50.0	8.76E+01	535	1.88E+03	308
(20)	300.0	50.0	5.91E+01	535	2.75E+03	304
(21)	300.0	100.0	1.26E+02	520	1.26E+03	305
(22)	400.0	50.0	2.84E+01	510	4.95E+03	276
(23)	400.0	100.0	5.78E+01	485	2.36E+03	281
(24)	500.0	100.0	2.81E+01	435	3.77E+03	244
(25)	750.0	100.0	1.94E+01	1025	8.68E+03	164
(26)	1000.0	100.0	8.74E+00	990	1.56E+04	137

TABLE.VI-4 CORRELATION OF RESISTIVITY AND LITHOLOGY

No.1

	Lithology	Grade humidity				Remark	
		dry	wet	capillary	saturate		
ASH	materials mud - clay		50-300		10-50	Q	h < 50 m
ASH	volcanic little compact	1000-4000	300-800	200-300	100-200	Q	
ASH	volcanic massive-regularly consolidate	≥ 1000	300-600			Q	
TUFF	Disturbed (Clay)	100-1000	10-100		10-50	T	
TUFF	Welded	1000-3000	500-1000		100-200	T	$1.00 \leq F \leq 5.00$ (m)
TUFF	Many fracture		200-500		100-200	T	$F \leq 1.00$ (m)
TUFF	Massive	> 3000				T	

TABLE VI-4 CORRELATION OF RESISTIVITY AND LITHOLOGY

No.2

	Lithology	Grade humidity				Remark	
		dry	wet	capillary	saturate		
LAVA	Andsite-Basaltic alteration block/ clay (regulate-small)		< 100	100-200		T	blocks 0.10<d≤1.00 (m)
	Andsite-Basaltic Fracture		300-600			T	
	Andsite-Basaltic many fracture		200-300		100-200	T	0.10≤F≤1.00 (m)
LIMESTONE	disturbed clayey		50-200			K	
	many fracture				100-200	K	F≤1.00 (m)
	massive	≥ 3,000			200-500	K	
	Materials clayey		5-50				
	Soil surface	> 100	5-50		50-200		

Q: Quaternary T: Tertiary K: Cretaceous

TABLE VI-5 SITE OF ELECTRICAL PROSPECTING

No.1

	NUMBER	ALTITUDE (m)	Current (m) Electrode spacing	Type of VES Curve	
NORTH AREA	SE-15	1440	1000	$\rho_1<\rho_2>\rho_3>\rho_4<\rho_5>\rho_6$	KQHK
	SE-19	1450	1900	$\rho_1>\rho_2<\rho_3$	H
	SE-20	1425	1000	$\rho_1<\rho_2>\rho_3<\rho_4$	KH
	SE-23	1460	1000	$\rho_1<\rho_2>\rho_3>\rho_4<\rho_5$	KQH
	SE-24	1475	1000	$\rho_1<\rho_2>\rho_3<\rho_4$	KH
	SE-29	1535	1900	$\rho_1<\rho_2>\rho_3<\rho_4$	KH
	SE-30	1485	1500	$\rho_1<\rho_2>\rho_3<\rho_4>\rho_5$	KHK
	SE-34	1520	1300	$\rho_1<\rho_2>\rho_3$	K
	SE-35	1484	1100	$\rho_1<\rho_2>\rho_3$	K
	SE-38	1405	1300	$\rho_1>\rho_2<\rho_3>\rho_4$	HK
	SE-47	1378	1500	$\rho_1<\rho_2>\rho_3>\rho_4$	KQ
SUB-TOTAL	11				
EAST AREA OF FAULT	SE-1	1425	1500	$\rho_1<\rho_2>\rho_3$	K
	SE-2	1360	1300	$\rho_1<\rho_2>\rho_3>\rho_4<\rho_5$	KQH
	SE-3	1365	1500	$\rho_1<\rho_2>\rho_3$	Q
	SE-4	1360	1000	$\rho_1<\rho_2<\rho_3>\rho_4$	AK

TABLE. VI-5 SITE OF ELECTRICAL PROSPECTING

No.2

	NUMBER	ALTITUDE (m)	Current (m) Electrode spacing	Type of VES Curve	
EAST AREA OF FAULT	SE-5	1485	1000	$\rho_1<\rho_2<\rho_3>\rho_4$	AK
	SE-6	1480	1500	$\rho_1>\rho_2<\rho_3>\rho_4>\rho_5$	HKQ
	SE-7	1450	800	$\rho_1<\rho_2>\rho_3<\rho_4$	KH
	SE-8	1480	1000	$\rho_1>\rho_2<\rho_3>\rho_4<\rho_5$	HKH
	SE-9	1500	600	$\rho_1<\rho_2>\rho_3<\rho_4>\rho_5$	KHK
	SE-10	1480	1000	$\rho_1>\rho_2<\rho_3>\rho_4$	HK
	SE-11	1390	1500	$\rho_1>\rho_2<\rho_3<\rho_4>\rho_5<\rho_6$	HAKH
	SE-12	1490	1500	$\rho_1>\rho_2<\rho_3>\rho_4<\rho_5$	HKH
	SE-13	1465	1900	$\rho_1>\rho_2<\rho_3<\rho_4$	HA
	SE-14	1395	1900	$\rho_1>\rho_2<\rho_3>\rho_4<\rho_5<\rho_6$	HKHA
	SE-15	1450	1000	$\rho_1<\rho_2>\rho_3<\rho_4>\rho_5<\rho_6$	KHKH
	SE-16	1408	1500	$\rho_1>\rho_2<\rho_3>\rho_4<\rho_5$	HKH
	SE-18	1525	1100	$\rho_1<\rho_2>\rho_3>\rho_4<\rho_5<\rho_6$	KQHA
	SE-21	1521	1500	$\rho_1<\rho_2<\rho_3>\rho_4<\rho_5$	AKH
	SE-22	1548	2000	$\rho_1<\rho_2<\rho_3<\rho_4>\rho_5$	AAK
	SE-25	1515	2000	$\rho_1<\rho_2>\rho_3$	K

TABLE. VI－5　SITE OF ELECTRICAL PROSPECTING

No.3

	NUMBER	ALTITUDE (m)	Current (m) Electrode spacing	Type of VES Curve	
EAST AREA OF FAULT	SE-26	1542	2000	$\rho_1<\rho_2>\rho_3<\rho_4>\rho_5$	KHK
	SE-27	1530	1500	$\rho_1<\rho_2>\rho_3$	K
	SE-28	1570	1500	$\rho_1<\rho_2<\rho_3$	A
	SE-31	1565	1600	$\rho_1<\rho_2>\rho_3$	K
	SE-32	1575	1000	$\rho_1<\rho_2>\rho_3$	K
	SE-33	1760	1500	$\rho_1<\rho_2>\rho_3<\rho_4$	KH
	SE-36	1510	2000	$\rho_1<\rho_2>\rho_3<\rho_4>\rho_5$	KHK
	SE-37	1475	1900	$\rho_1>\rho_2<\rho_3>\rho_4$	HK
	SE-39	1868	800	$\rho_1<\rho_2>\rho_3$	K
	SE-40	1868	500	$\rho_1<\rho_2>\rho_3$	K
	SE-41	1670	1700	$\rho_1<\rho_2>\rho_3<\rho_4>\rho_5$	KHK
	SE-42	1480	1500	$\rho_1>\rho_2<\rho_3>\rho_4$	HK
	SE-43	1420	1400	$\rho_1>\rho_2<\rho_3>\rho_4$	HK
	SE-44	1615	1500	$\rho_1<\rho_2>\rho_3<\rho_4$	KH
	SE-45	1478	1400	$\rho_1>\rho_2<\rho_3>\rho_4>\rho_5$	HKQ

TABLE.VI - 5 SITE OF ELECTRICAL PROSPECTING

No.4

	NUMBER	ALTITUDE (m)	Current (m) Electrode spacing	Type of VES Curve	
EAST AREA OF FAULT	SE-46	1400	700	$\rho_1<\rho_2<\rho_3<\rho_4$	QQ
	SE-48	1875	1300	$\rho_1<\rho_2<\rho_3<\rho_4$	KH
	SE-49	1740	1300	$\rho_1<\rho_2<\rho_3<\rho_4<\rho_5<\rho_6$	AKHK
	SE-50	1275	1100	$\rho_1<\rho_2<\rho_3<\rho_4$	KQ
	SE-51	1490	1200	$\rho_1<\rho_2<\rho_3<\rho_4$	KH
	SE-52	1455	700	$\rho_1<\rho_2<\rho_3$	K
	SE-53	1395	500	$\rho_1<\rho_2<\rho_3$	K
	SE-54	1545	800	$\rho_1<\rho_2<\rho_3$	K
	SE-55	1520	1200	$\rho_1<\rho_2<\rho_3<\rho_4<\rho_5$	AKH
	SE-56	1520	1000	$\rho_1<\rho_2<\rho_3$	K
	SE-57	1495	2000	$\rho_1<\rho_2<\rho_3$	K
	SE-58	1475	1500	$\rho_1<\rho_2<\rho_3$	K
	SE-59	1395	1500	$\rho_1<\rho_2<\rho_3<\rho_4$	KH
	SE-60	1435	1700	$\rho_1<\rho_2<\rho_3<\rho_4$	KH
	SE-61	1460	2000	$\rho_1<\rho_2<\rho_3$	K
TOTAL	61				

CHAPTER VII

TEST BORING

7.1 Object:

Test boring is implemented at 5 points in consideration of ground water potentiality resulting from the hydrogeologic study and electric logging. The 6 sites are shown in FIG. VII-1. Three of the wells are production wells and the others are observation wells.

7.1.1 Site Section:

Test boring sites were selected on the basis of the following.

(1) Choice of Drilling Site Nº 1 (12")

Drilling site Nº 1 (altitude 1,410 m above sea level) is located about 60 m southwest of electrical prospecting - site SE-1. The reasons for choosing this drilling site are as follows:

a) The interpretation for electric prospecting site SE-1 indicated a rising and falling curve and from this, existence of an aquifer can be expected, even though the basement has not yet been analyzed.

b) From a hydrogeological viewpoint, the chosen site corresponds to a confluence of subterranean streams, and a good groundwater artery can be expected.

c) About 150 m northwest of the chosen site is a well (altitude 1,390 m above sea level) with a water level of 1,288 m and a pump-up volume of 24 l/s.

The type of rock is mudstone with limestone intercalation.

d) Urbanization is accelerating in zone 18 and the area is a water shortage area.

e) There are outcrops of limestone in the westward vicinity of the chosen site. The fault is well developed and there are many fractures. Consequently, it is thought that the site is located in an area where the geological units have a good permeability.

(2) Choice of Drilling Site Nº 2 (12")

Drilling site Nº 2 (altitude 1,537 m above sea level) is located about 600 m south of electrical prospecting site SE-36. Reasons for choosing this drilling site are as follows:

a) The recharge basin of this site is the San Jose Pinula plateau. From a topographical viewpoint, this is an uplifted zone. A groundwater artery is estimated to run in the northwest-northeast direction in the vicinity and the drilling site is situated above the same.

b) The pyroclastic material layer in the vicinity is judged to be thin on the basis of the interpretation of the results for electrical prospecting in SE-36. It is projected that in the lower portion of the pyroclastic material, semimenation of lava (andestic-basaltic) and welded tuff which is thought to be a saturated layer occurs. Fissures occur in the welded tuff and lava due to fault and joint action and therefore the layer is considered to form a good aquifier.

c) There is no well in Canalitos and the inhabitants rely on pumped-up spring water for their drinking supply. It is necessary to check the geological conditions and groundwaer basin reserve through drilling site Nº 2.

(3) Choice of Drilling Site Nº 3 (12")

Drilling site Nº 3 (altitude 1,285 m above sea level) is located about 1,100 m north-east of electrical prospecting site SE-1 along Highway Nº 9. Reasons for choosing this drilling site are as follows.

a) Drilling site Nº 1 is in a topographically uplifted zone whereas drilling site Nº 3 is in a submerged zone. It is necessary to check the water level for both sites.

b) Drilling site Nº 3 is situated at the confluence of groundwater arteries.

c) It is necessary to check the geological conditions and groundwater basin reserve at the site.

The outcome of the pumping test will be reported in the Final Report.

7.1.2 Drilling Method:

The drilling method is an adapted "rotary type" and was selected for the following reasons:

(1) The drilling depth is assumed to be at approximately 200-300 m and many cases of trouble have been reported from nearby areas for implementation.

2) Implementation is scheduled to be performed by contract with local companies, and the rotary method is the method generally used in Guatemala because of its advantages over the others.

TABLE VII - 1

GENERAL FEATURES OF TEST BORING

Well	Construction Period	Object	Drilling speed	Total Depth	Static water level	Ground level	Comment
Nº 1	1985.9-30-12-4 (17-1/2")	Production	180 m: 30cm/h 180 m: 50cm/h	300 m	GL - 180.70	1,410 m	
Nº 2	1985-12-11 1986.2.12	Production	170cm/h	300 m	GL - 95.80	1,537 m	30m, 70m 120m, faulting
Nº 3	1986.1.3-3.3	Production	140 m: 20cm/h limestone: 100cm/h	300 m	GL - 63.00	1,285 m	
Nº 4	1985.10.10-10.31 (12-1/4")	Observation	110cm/h	220 m	GL - 110.00	1,410 m	
Nº 5	1985.12.5-12.14 (12-1/4")	Observation	110cm/h	120 m	GL - 7.00	1,381 m	
Nº 6	1986.1.6-1.20 (12-1/4")	Observation	300cm/h	300 m	GL - 170.00	1,452 m	220 - lime- tone.